THE EFFECTS OF *SUTHERLANDIA FRUTESCENS* AND FUMONISIN B_1 ON JURKAT CELLS

Keiron Audain

Submitted in fulfilment of the academic requirements for the degree of

Master of Medical Science

Health Sciences

University of KwaZulu Natal

Durban

South Africa

October 2011

ABSTRACT

The medicinal plant *Sutherlandia frutescens* (SF) is commonly consumed in South Africa, and is traditionally applied to a range of ailments. Yet its popularity stems from the use of SF as a cancer treatment. This plant contains a range of active compounds including L-canavanine (L-CAV), D-pinitol and gamma (γ)-aminobutyric acid, all of which contribute to the therapeutic properties of SF. It is also endorsed by the South African Ministry of Health as a supplementary treatment for HIV/AIDS.

Maize is the staple crop of South Africa, and can be frequently contaminated by the mycotoxin fumonisin B_1 (FB_1). The mycotoxin is linked to an extensive list of livestock diseases. Although little is known about its role in human disease, FB_1 has been epidemiologically linked to oesophageal cancer in South Africa.

Both SF and FB_1 have been shown to promote apoptosis, and the effect(s) of consuming both in combination is currently unknown.

The principle aim of this study was to determine whether SF and FB_1 had either synergistic or antagonising effects in combination, by investigating immune cell toxicity Jurkat cells. Apoptotic parameters such as caspase activation, mitochondrial depolarisation, phosphatidylserine (PS) externalisation and ATP quantification were analysed. Levels of caspase activation were highest in cells treated with SF only (caspase-3: 86.79 RLU, no significance compared to other treatments; caspase-8: 40.1 RLU, significance compared to other treatments [$p<0.05$]; caspase-9: 11.07 RLU, significance compared to FB_1 and control treatments [$p<0.05$]). ATP levels were significantly highest in SF-treated cells compared to other treatments (8.17 RLU, [$p<0.05$]). Mitochondrial depolarisation was also highest in SF-treated Jurkat cells at 18.5% depolarisation with no significance compared to other

treatments, however PS externalisation were significantly lower in SF-treated cells compared with other treatments (3.69% [$p<0.05$]).

Oxidative stress parameters were also investigated, including thiobutyric acid reactive species (TBARS), Glutathione (GSH) and Reactive Nitrogen Species (RNS) assays. TBARS levels were significantly higher in FB_1 treated cells (OD 1.95, [$p<0.05$]) compared to SF and control. Glutathione and RNS levels were also lowest in FB_1.treated cells.

The data suggests that SF induces apoptosis, characteristic of its nature as an anti-cancer treatment, and FB_1 induces oxidative stress, which is characteristic of its carcinogenic properties. Based on this preliminary study, it appears that FB_1 and SF both synergises and antagonises the other in combination, yet further investigation is needed into its effects *in vivo*.

DECLARATION

This study represents the original work by the author and has not been submitted in any form to another university. The use of work by others has been duly acknowledged in the text.

The research described in this study was carried out in the Discipline of Medical Biochemistry, Faculty of Health Sciences, University of KwaZulu-Natal, Durban, under the supervision of Prof. A.A. Chuturgoon.

.....

K.A. Audain

ACKNOWLEDGEMENTS

Prof. A.A. Chuturgoon

Thank you for giving me the opportunity to undergo this study. Your guidance, support and encouragement throughout the past year and even before I came to South Africa will forever be remembered.

Dr. D. Moodley

Thank you for your assistance with structuring this study and planning my experiments. Your input has been invaluable in making this project what it has become.

Alisa Phulukdaree

Thank you for setting such high standards in the lab, which has helped me to achieve both my project and personal goals.

My lab colleagues

Thanks for all the help with reagents, protocols and general guidance. I wish you all success in future endeavours.

My mother

Without your unconditional love, support, advice and encouragement, this would not have been possible. I owe all my achievements to you.

ABBREVIATIONS

^{o}C	Degrees Celsius
µg	Microgram
µL	Microlitre
µM	Micrometre
ΔΨm	Mitochondrial Membrane Potential
AIDS	Acquired Immune Deficiency Syndrome
AIF	Apoptosis Inducing Factor
ANOVA	Analysis of Variance
Annexin-V-FITC	Annexin-V-Fluorescein Isothiocyanate
Apaf-1	Apoptotic Protease-Inducing Factor-1
APS	Ammonium Persulphate
Asp	Aspartate
ATP	Adenosine triphosphate
BCA	Bicinchoninic Acid
BSA	Bovine Serum Albumin
Ca^{2+}	Calcium ion
CARD	Caspase Recruitment Domain
Caspase	Cysteine-dependent aspartate-specific protease
cFLIP	FLICE Inhibitory Protein
cm	Centimetre
CO_2	Carbon Dioxide
Cu^{2+}	Copper Ion
$Cu(II)SO_4$	Copper Sulphate
Cys	Cysteine
DD	Death Domain

DED	Death Effector Domain
dH_2O	De-ionized water
DISC	Death-Inducing Signalling Complex
DMSO	Dimethyl Sulphoxide
DNA	Deoxyribonucleic Acid
DNase	Deoxyribonuclease
EDTA	Ethylenediaminetetraacetic acid
ER	Endoplasmic Reticulum
ERK1/2	Extracellular Signal Regulated Kinases 1 and 2
EtBr	Ethidium Bromide
EtOH	Ethanol
FADD	Fas-associated Death Domain
$FADH_2$	Flavin Adenine Dinucleotide
Fe^{3+}	Iron (III)
FACS	Fluorescence Activated Cell Sorting
FCS	Foetal Calf Serum
FL	Fluorescence
FSC	Forward Light Scatter
GABA	Gamma (y)-Aminobutyric Acid
GSH	Glutathione
HCO^-_3	Hydrogen Carbonate
HIV	Human Immunodeficiency Virus
h	Hour
HRP	Horse Radish Peroxidase
IAP	Inhibitor of Apoptosis Protein
IM	Inner Mitochondrial Membrane
iNOS	Inducible Nitric Oxide Synthases

JNK	Jun N-terminal Kinase
K^+	Potassium Ion
KCl	Potassium Chloride
K_2EDTA	Dipotassium Ethylenediaminetetraacetic Acid
KH_2PO_4	Potassium Dihydrogen Phosphate
L-ARG	L-Arginine
L-CAV	L-Canavanine
LMPA	Low Melting Point Agarose
M	Molar
mA	Milliampere
MAPK	Mitogen Activated Protein Kinase
mg	milligram
min	minutes
ml	millilitre
mm	millimetre
mM	millimolar
MTT	Methylthiazol Tetrazolium
Na^+	Sodium Ion
Na_2EDTA	Disodium Ethylenediaminetetraacetic Acid
NaCl	Sodium Chloride
NADH	Reduced Nicotinamide Adenine Dinucleotide
NADPH	Reduced Nicotinamide Adenine Dinucleotide Phosphate
NaOH	Sodium Hydroxide
NK	Natural Killer
NO	Nitric Oxide
OM	Outer Mitochondrial Membrane

PBS	Phosphate Buffered Saline
PCD	Programmed Cell Death
Phe	Phenylalanine
PI	Propidium Iodide
PKC	Protein Kinase C
P/S	Penicillin/Streptomycin
PS	Phosphatidylserine
PT	Permeability Transition
PTPC	Permeability Transition Pore Complex
PVDF	Polyvinylidene Fluoride
RBC	Red Blood Cell
RNA	Ribonucleic Acid
ROS	Reactive Oxygen Species
rpm	revolutions per minute
RPMI	Roswell Park Memorial Institute
RT	room temperature
SCGE	Single Cell Gel Electrophoresis
SDS	Sodium Dodecyl Sulphate
SDS-PAGE	SDS – Polyacrylamide Gel Electrophoresis
SEM	Standard Error of Mean
Smac/DIABLO	Second mitochondria-derived activator of caspase/direct IAP-binding protein with low pI
SMase	Sphingomyelinase
SSC	Side Light Scatter
tBid	truncated Bid
TCA	Tricarboxylic Acid
TEMED	Tetramethylenediamine

TNF	Tumour Necrosis Factor
TNFR1/2	Tumour Necrosis Factor Receptor 1 and 2
TRADD	TNF-Receptor Death Domain
TRAIL	Tumour Related Apoptosis inducing Ligand
tRNA	Transfer Ribonucleic Acid
TBARS	Thiobutyric acid reactive species
TBS	Tris-Buffered Saline
TTBS	Tween-Tris Buffered Saline
UV	Ultraviolet
V	Volts
VDAC	voltage-Dependent Ion Channel

TABLES

CHAPTER 2

CHAPTER 3

CHAPTER 4

FIGURES

CHAPTER 1

CHAPTER 2

CHAPTER 3

CHAPTER 4

CHAPTER 5

TABLE OF CONTENTS

CHAPTER 5: SPECTROPHOTOMETRIC ANALYSIS OF REACTIVE NITROGEN AND OXYGEN SPECIES IN FUMONISIN B_1 AND *SUTHERLANDIA FRUTESCENS* TREATED JURKAT CELLS

INTRODUCTION

Fumonisin B_1 (FB_1) is a secondary metabolite produced by the ubiquitous soil fungus *Fusarium verticillioides,* a widespread maize crop infection (Schwerdt *et al.* 2008). Maize comprises a substantial portion of the South African diet and consumption of FB_1-contaminated foods is considered a risk factor for human oesophageal cancer in parts of South Africa where the disease has a high incidence (Dragan, *et al.* 2001, Visconti, *et al.* 1995). Mycotoxins can remain stable at high temperatures, and the possibility exists for mycotoxins such as FB_1 to be present in maize and other grains even after cooking and food processing (Bhatnagar, *et al.* 2002). In a survey conducted in KwaZulu Natal, South Africa, FB_1 contamination was observed in 8 out of a total 28 samples of cooked maize (Chulele, *et al.* 2001).

South Africa has an exceptionally high disease burden in relation to infectious diseases such as human immunodeficiency virus (HIV) and tuberculosis (TB), as well as non-communicable disease such as various cancer types. Traditional healers and the use of medicinal plants are an integral part of healthcare systems throughout Africa, and in South Africa up to 27 million people are reported to use traditional medicine, the trade of which is estimated to contribute approximately US $400 million annually towards the national economy (Mander, *et al.* 2007).

Sutherlandia frutescens (SF), referred to as “cancer bush” in English, is a member of the Leguminosae family, a shrub endemic to Southern Africa (van Wyk 2008). The popularity of SF is mainly due to its medicinal use against a range of diseases, most notably cancer, (van Wyk, 2008) and it is currently endorsed by the South African Ministry of Health as a supplementary treatment for HIV/AIDS (Mills 2005).

Both FB1 and SF have reported apoptotic activity. Apoptosis is postulated to be the mechanism behind the anti-cancer properties of SF (Chinkwo, *et al.* 2005). L-canavanine (L-CAV) found in extracts of SF, is a non-protein structural analogue of L-arginine (L-ARG), capable of replacing L-ARG to form non-functional canavanyl proteins (Mills, 2005). This in turn disrupts the synthesis of cellular nitric oxide (NO) (Akaogi, *et al.* 2006; Riganti, *et al.* 2003), as NO production involves the conversion of L-ARG to L-citrulline via inducible nitric oxide synthase (iNOS). Nitric oxide has been shown to regulate apoptosis via a process known as S-nitrosylation (Liu, *et al.* 2010, Iyer, *et al.* 2008).

Apoptotic markers such as DNA fragmentation, morphological changes and chromatin condensation were observed in neoplastic cervical carcinoma cells treated with aqueous extracts of SF (Chinkwo, *et al.* 2005).

It is hypothesised that FB_1 induces apoptosis via an inhibitory effect on ceramide synthase, the enzyme responsible for sphingolipid synthesis (Ribiero, *et al.* 2010). Sphingolipids are an important component of plasma membranes, and are associated with regulating cell growth and differentiation. The sphingoid-like lipophilic backbone of FB_1 is structurally analogous to sphinganine, a substrate involved in sphingolipid metabolism (Yin, *et al.* 1998), which suggests that FB_1 may possess the ability to block the action of ceramide synthase by competitive inhibition (Ribiero, *et al.* 2010).

Despite this hypothesis, FB_1 has also been observed to exhibit proliferative effects. Proliferative or apoptotic effects of FB_1 vary according to the cell type. The cell viability of rabbit kidney cells (RK13) diminished after treatment with nanomolar concentrations of FB_1 for 24 hours (Rumora, 2002). In contrast, the Jurkat T cell line treated with increasing concentrations of FB_1 (0-150 μM) for the same time period showed a consistent dose-dependent increase in proliferation, reaching a plateau at 80 μM of FB_1 (Luongo, *et al.* 2006).

Despite a proliferative action in T cells, FB_1 has also demonstrated immune suppressing effects in human immunocytes extracted from carcinoma patients, Dose-dependent reductions in cell viability was observed when leukocytes from breast and oesophageal cancer patients were exposed to FB_1 (Odhav, *et al.* 2008).

Previous studies linked FB_1 to oxidative stress (Abel and Gelderblom, 1998; Rumora, *et al.* 2007). Cellular membranes are postulated to be the main target for the cytotoxic effect of FB_1, and evidence for its role in lipid peroxidation has been presented, including dose-dependent increases in reactive species generation in various cell lines treated with FB_1 (Abel and Gelderbloom, 1998; Stockmann-Juvala, *et al.* 2004). Still, the mechanism behind its action remains largely unknown.

In contrast, SF has been linked to antioxidant activity, owing to its phenolic and flavonoid constituents. Fernandes, *et al.* (2004) demonstrated that SF may possess superoxide and hydrogen peroxide (H_2O_2) scavenging properties in neutrophils, which were observed at concentrations as low as 10µg/mL.

The links between FB_1 exposure, immune suppression, apoptosis and/or oxidative stress is not yet fully understood. Due to the high consumption of maize and maize products in South Africa, and the popularity of SF as a traditional medicine, it is possible that both SF and FB_1 are frequently ingested in combination. This study aims to investigate the effects of exposure to both SF and FB_1 on immune cells, by measuring apoptotic and oxidative stress parameters in the human acute T cell leukaemia Jurkat cell line (a model of T lymphocytes) pre-treated with the IC_{50} concentration of FB_1 and SF.

AIM AND OBJECTIVES

The aim of this study was to expose the human acute T cell leukaemia Jurkat cell line to *Sutherlandia Frutescens* (SF) and Fumonisin B1 (FB_1), to determine any possible synergism or antagonism.

Apoptotic and oxidative stress parameters were measured in Jurkat cells pre-treated with the IC_{50} concentration of FB_1 and SF.

These parameters included assessment of mitochondrial membrane potential (MMP), phosphatidylserine (PS), metabolic activity, glutathione antioxidant response, and lipid peroxidation in FB_1 and SF-treated Jurkat cells.

CHAPTER 1: LITERATURE REVIEW

1.1 *SUTHERLANDIA FRUTESCENS*

The use of medicinal plants is an integral part of healthcare systems in Africa. In South Africa, up to 27 million people are reported to use traditional medicine, the trade of which is estimated to generate R2.9 billion (approx US $400 million) annually towards the national economy (Mander, *et al.* 2007). *Sutherlandia frutescens* is one of the best known therapeutic plants in Southern Africa, and has long been incorporated in the medicinal framework across the region.

Sutherlandia frutescens, a perennial shrub that grows up to 2 ½ metres in length, is an indigenous member of the Leguminosae family. It is identified by its oval, oblong shaped leaves and light, but bright red tubular flowers. A number of subspecies exist and are located along the coastal areas of Southern Africa (van Wyk and Albrecht, 2008).

Traditionally, SF was applied broadly to a range of ailments, most notably diabetes, fevers, stomach ailments, and general stress. Its popularity however, stems from its use as a cancer treatment, hence being given the name –cancer-bush" (*unwele* in isiZulu; *kankerbos* in Afrikaans).

Scientific and commercial interest in SF has increased considerably over the past decade, mainly due to its association with not only cancer, but also HIV/AIDS. In South Africa, SF is officially endorsed by the Ministry of Health as a supplementary treatment for HIV/AIDS (Mills *et al.* 2005). The company Phyto Nova (Pty) Ltd is the main large-scale cultivator of SF, and manufactures a 300 milligram (mg) tablet containing stem and leaf extracts of the plant.

The leaves of SF contain the non-protein amino acid L-canavanine (L-CAV), a structural analogue of L-arginine (L-ARG). As a result of its structural similarity, L-CAV is capable of inhibiting the action of L-ARG-utilising enzymes such as inducible nitric oxide synthase (iNOS or type II) and arginase. iNOS synthesises a sustained amount of nitric oxide (NO) over prolonged periods and produces the highest quantity of NO compared to other members of the NOS family. Nitric oxide is an inert, free radical gas critically involved in apoptosis via mitogen-activated protein kinases (MAPK) activation. The up-regulation of NO is controlled by the release of tumour necrosis factor- α (TNF-α) and other signalling molecules that increase NO synthesis (Kim, *et al.* 2001).

The inhibition of iNOS can lead to the disruption of NO synthesis, as cellular NO production involves the conversion of L-ARG to L-citrulline via iNOS (Akaogi, *et al.* 2006, Riganti, *et al.* 2003).

Nitric oxide has been implicated in tumour cell growth promotion by inducing cell proliferation, suggesting a regulatory role for NO in apoptosis. Hence, NO may possess concentration-dependent pleiotropic functions (Iyer, *et al.* 2008).

The role of nitric oxide in apoptotic regulation occurs via S-nitrosylation, which is defined as ~~–t~~he reversible coupling of a nitroso moiety to a reactive cysteine thiol, (which) leads to the formation of S-nitrosothiol" (Iyer, *et al.* 2008). S-nitrosylation of pro-apoptotic proteins results in both the induction and the inhibition of apoptosis. For example, the S-nitrosylation of caspase-3, caspase-8 and caspase-9 inhibits their enzymatic activity, causing an anti-apoptotic effect. In contrast, S-nitrosylation can degrade the anti-apoptotic FLICE Inhibitory Protein (FLIP) protein, which in turn promotes apoptosis (Iyer, *et al.* 2008).

Additional anti-cancer properties attributed to L-CAV is owed to its primary metabolite L-canaline. L-canaline is catalysed by the enzyme arginase, and was found to be cytotoxic

towards peripheral blood mononuclear cells (PBMCs) (Bence, *et al.* 2002). L-CAV can also bind to arginyl tRNA synthetase during protein synthesis, to form non-functional canavanyl proteins, which has both anti-cancer and antiviral properties (Mills, *et al.* 2005; Akaogi, *et al.* 2006).

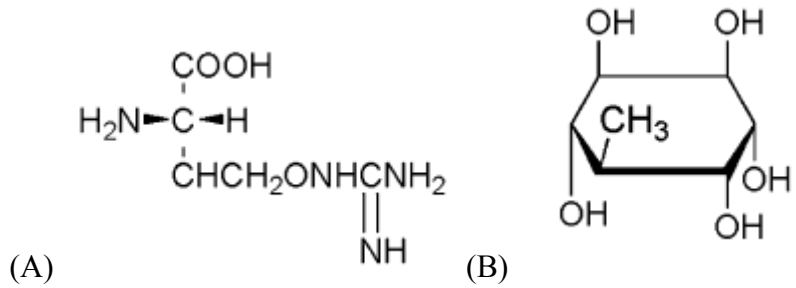

Figure 1.1: (A) Structure of L-canavanine (L-CAV); (B) Structure of D-Pinitol.

The leaves of SF also contain D-Pinitol, a 3-methoxy cyclitol analogous to D-chiroinositol. D-Pinitol is proposed to exert insulin-like properties by lowering blood sugar levels, and increasing glucose availability for use in cell metabolism. It was observed that basal glucose uptake in cultured L6 muscle cells increased upon treatment with D-Pinitol (10^{-3} M) (Bates, *et al.* 2000). Further links to its insulin-like effects stems from the fact that D-Pinitol is structurally similar to inositol phosphates involved in insulin signalling via PI3K and protein kinase B (PKB) (Holman & Kasuga, 1997). This, in addition to its role in boosting creatine retention in muscle cells, links SF with a possible role in the treatment of wasting in both AIDS and cancer patients (Greenwood, *et al.* 2001).

Sutherlandia contains a range of other phyto-active compounds such as phenols, flavonoids and *Triterpenoid saponins*, which has linked it with antioxidant activities. Fernandes *et al.* (2004) showed SF possesses potent superoxide and hydrogen peroxide scavenging properties in neutrophils at relatively low concentrations. The ROS scavenging properties of SF may account for its effects and use as an anti-inflammatory agent, however the mechanism behind its antioxidant activity as yet remains unknown (Fernandes, *et al.* 2004).

The endorsement and commercial availability of SF is not yet in accordance with the amount of scientific data currently existing on the plant, compared to other medicinal plants. Few studies have been conducted on SF usage, particularly with respect to contraindications with drug therapy and food contaminants.

1.2 FUMONISIN B_1

The mycotoxin FB_1 is a secondary metabolite produced by the ubiquitous soil fungus *Fusarium verticillioides* (formerly known as *Fusarium Monoliforme*) and has been isolated from a number of agricultural crops and cereals, particularly maize. Fumonisin B_1 is associated with an extensive list of diseases in livestock, including leukoencephalomalacia in horses, pulmonary oedema in pigs, and hepatic cancer in rats (Schwerdt, *et al.* 2009). As a result, research into its containment is considered to be of economic importance. The role of FB_1 in human disease however, leaves room for much needed investigation.

Isolated strains of the *Fusarium verticillioides* fungus from European grown maize have been reported to produce up to 4mg/g of FB_1 and FB_2 (Visconti, *et al.* 1995). Investigations into the prevalence of fumonisin contamination of corn-based foods in Southern California found the mycotoxin present in all 38 samples examined, at a median concentration of 231ng/g

(Dvorak, *et al.* 2008). Mycotoxins can remain stable despite temperature changes, and the possibility exists for mycotoxins such as FB_1 to remain present in maize and other grains subsequent to cooking and food processing (Bhatnagar, *et al.* 2003). A survey conducted in KwaZulu Natal, South Africa showed the presence of FB_1 in 29% out of a total of 28 cooked maize samples (Chulele, *et al.* 2001). Fumonisin B_1 has been epidemiologically linked to oesophageal cancer (Dragan, *et al.* 2001, Visconti, *et al.* 1995), yet the mechanism behind its proposed carcinogenicity has not yet been fully elucidated.

Over 15 fumonisin isomers exist, and FB_1 appears to be most abundantly present. Fumonisin B_1 contains 10 stereocenters, which allows for the possibility for 1024 different stereochemical structures. Fumonisin B_1 belongs to the aminopolycarboxylic acid family, and bears a strong structural similarity to sphinganine, owing to its hydroxygroups, aminogroup and a 20-carbon lipophilic backbone (Yin, *et al.* 1998).

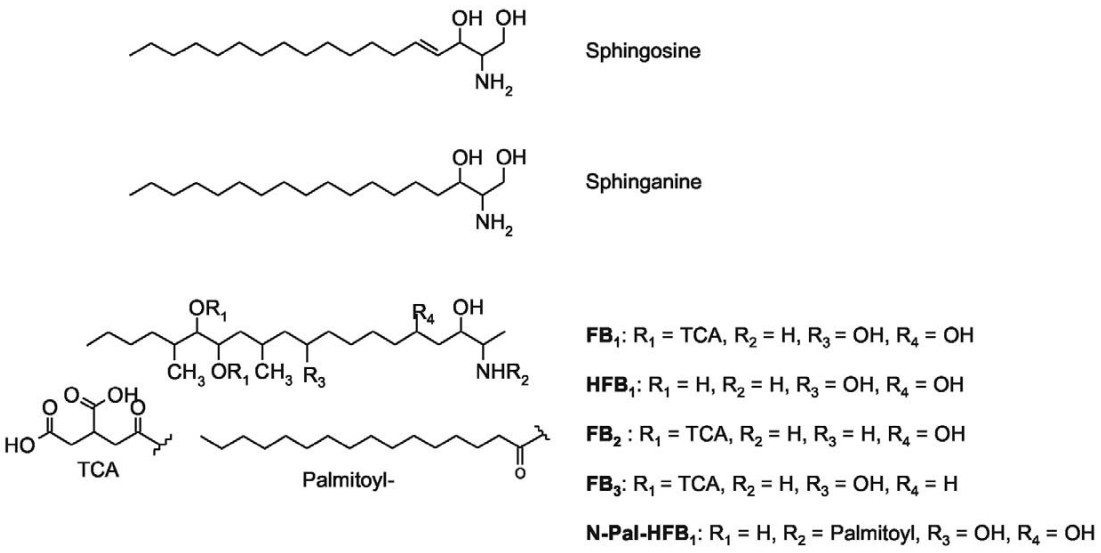

Figure 1.2: Structures of sphingosine, sphinganine, FB1, hydrolyzed FB1 (HFB1), FB2, FB3, and palmitoyl-hydrolyzed FB1 (N-Pal-HFB1) (Seefelder, 2003).

Sphinganine is a sphingoid base substrate that is converted to a sphingolipid product via the action of ceramide synthase, the enzyme responsible for sphingolipid metabolism. The structural similarity of FB_1 enables FB_1 to prevent the binding of sphinganine to ceramide synthase via competitive inhibition, thus inhibiting ceramide synthesis (Ribiero, *et al.* 2010). Sphingolipids are a significant component of plasma membranes, and are important signalling molecules associated with regulating signal transduction pathways such as cell proliferation, cytokine induction and apoptosis (Luongo, *et al.* 2006). The carcinogenicity of FB_1 has thus been attributed to cell signalling disruption owing to the ability of FB_1 to inhibit sphingolipid synthesis.

The sphingolipid ceramide is produced via cytokine activation and sphingomyelin (SM) hydrolysis, catalysed by sphingomyelinase (SMase). Sphingoyelin is also a member of the sphingolipid species, and is abundantly present in cell membranes, carrying important structural and functional properties (Liu, *et al.* 1997). The enzyme SMase is linked to TNFα-induced apoptosis, which will be discussed later. Ceramide is considered to be an important apoptotic regulator, and has been associated with the induction of nitro-oxidative stress, through its stimulation of reactive species $O_2^{\cdot}$ and NO. Therefore the inhibition of this ceramide synthesis by FB_1 should contribute to limiting the presence of reactive species, and as an extension to reduce oxidative damage (Cuzzocrea, *et al.* 2008). However, FB_1 has been linked to the induction of oxidative stress (Rumora, *et al.* 2007), and evidence has been presented to support a role for FB_1 in lipid peroxidation (Abel and Gelderblom, 1998; Stockmann-Juvala, *et al.* 2004). Lipid peroxidation is defined as the induction of cyclic lipid degradation of polyunsaturated fatty acids. Lipid Peroxidation alters the lipid structure of cell membranes, thus impacting on the fluidity of the membrane, leading to loss of function and the destabilisation of membrane-bound receptors and enzymes (Winrow, *et al.* 1993). Early

stages of lipid peroxidation can be measured by electron spin resonance (ESR) oximetry, which measures the concentration of aqueous molecular oxygen in liposomes as well as oxygen uptake. Fumonisin B_1 may contribute to lipid peroxidation by increasing molecular oxygen transport close to the surface of cell membranes, which may potentially accelerate oxidative reactions and ROS generation in the hydrophobic region of the membrane (Yin, et. al 1998).

When the effect of FB_1 on lipid peroxidation in egg yolk phosphatidylcholine (EYPC) bilayers was demonstrated, Yin *et al.* (1998) observed that FB_1 disrupted membrane ordering and increased oxygen transport as well as membrane permeability. It was suggested that membrane damage via lipid peroxidation and other free radical processes could also lead to oxidative damage of DNA (Yin, et. al. 1998). Stockmann-Juvala *et al.* (2004) showed a dose- and time-dependent increase in lipid peroxidation and ROS generation in U-118MG glioblastoma cells treated with FB_1 (Stockmann-Juvala, et al 2004).

Fumonisin B_1 has been previously described as non-genotoxic; owing to the fact that studies were not able to find DNA damage both *in vivo* and *in vitro* DNA repair assays in primary rat hepatocytes (Gelderblom, *et al.* 1992). Yet, when Rumora *et al.* (2002) measured the ability of FB_1 treated rabbit kidney cells (RK13) to induce micronuclei as a marker for genotoxicity, a significant increase in micronucleus was observed, albeit time and dose-dependent (Rumora, *et al.* 2002). In a separate analysis, the mechanism behind the genotoxic effect of FB_1 was attributed to its ability to induce oxidative stress (Abel, *et al.* 1998).

The proliferative and/or apoptotic effects of FB_1 appear to vary among different cell types. The cell viability of RK13 cells diminished after treatment with nanomolar concentrations of FB_1 for 24h (Rumora, 2002), yet in contrast, the Jurkat T cell line treated with increasing

concentrations of FB_1 (0-150 μM) for the same time period showed a consistent dose-dependent proliferation increase at low doses, finally reaching a plateau at 80 μM FB_1 (Luongo, *et al.* 2006). In spite of the cell proliferative activity in the Jurkat T cell line, FB_1 has also contributed to T-cell suppression in human patients. A dose-dependent reduction of human leukocytes was reported in oesophageal and breast cancer patients exposed to FB_1 (Odhav, *et al.* 2008).

1.3 TUMOUR NECROSIS FACTOR- α

Cytokines are proteins that act as chemical messengers between cells. They are produced by white blood cells and are capable of either stimulating or inhibiting the growth and activity of various immune cells, thus effectively playing a role in immune and inflammation regulation (Odhav, *et al.* 2008).

The cytokine TNF-α plays an instrumental role in growth modulation and differentiation in a range of cell types. It is involved in inflammatory responses, and is also linked to immune function regulation, owing to its pleiotropic properties.

Additionally, evidence has linked TNF-α to a range of therapeutic activities, including infection and tumour resistance development, embryonic development and sleep regulation (Idriss and Naismith, 2000).

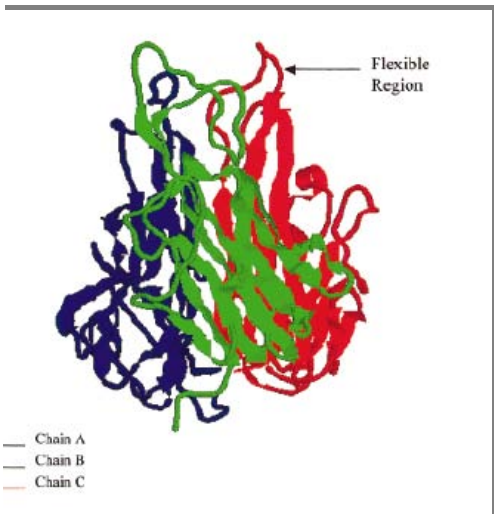

Figure 1.3: Ribbon diagram showing the ~~"~~one-shaped" TNFα trimer (Idriss and Naismith, 2000).

Cellular responses are signalled by TNF-α binding to cell surface receptors TNFR1 (or p55) and TNFR2 (or p75/80). A distinct role is played by TNF-α in death receptor-mediated apoptosis, via its ability to bind and cluster high-affinity receptors on cell membranes.

Although the binding of TNF-α to TNFR-2 has been reported to induce insufficient cytotoxicity to promote apoptosis (Idriss and Naismith, 2000), TNFR2 receptor expression is known to occur in activated T cells, and can contribute to T-cell homeostasis either through apoptotic or cell proliferative pathways (Puga, et. al 2005; Vandenabeele, *et al.* 1995). Also, T cells can provide informative data on TNFR2, owing to their possession of the biochemical machinery required to regulate TNFR2 expression.

Tumour Necrosis Factor-α binds to either TNFR1 or TNFR2 and the complex is internalized via clathrin-coated pits, and degraded within secondary lysosymes. This process activates a number of secondary proteins including transcription factors NF-κB and AP-1, MAP Kinases ERK-1 and ERK-2, and cysteine proteases, otherwise known as caspases. A range of cellular responses are also invoked, as in the case of inflammatory gene expression, and ROS/RNS generation.

In fact, TNF-α is linked to multiple gene expression such as IL-2 receptor, TNFR-associated factor 1 and FAS associated death domain like interleukin-1–converting enzyme inhibitory protein; all of which are the result of TNF-α activation of NF-κB, which is both redox sensitive and pro-inflammatory. Both TNFR1 and TNFR2 contain intracellular death domains (DD), which are instrumental in TNF-α-mediated apoptosis. These DD are responsible for caspase activation, particularly caspase-8, which is recruited to the activated receptor by adaptor proteins such as TRADD and FADD, which are discussed in the next section (Idriss and Naismith, 2000).

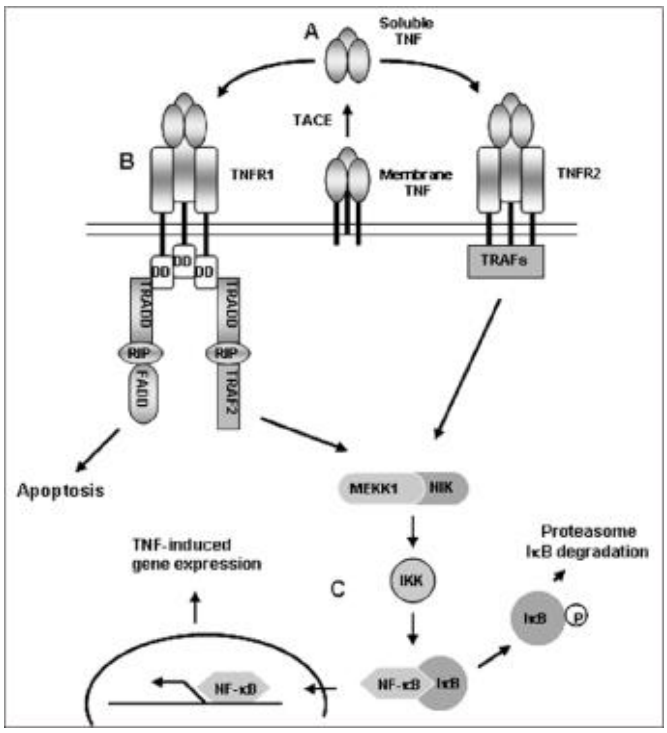

Figure 1.4: TNF signalling pathways involved in apoptosis (Rahman, *et al.* 2009).

The MAPKs are intracellular signalling pathways triggered in response to extracellular stimuli. MAPKs are released in response to an array of stimuli, and its signalling pathways play a fundamental role in eukaryotic gene expression, including cell growth, differentiation and apoptosis. MAPKs control gene expression via their ability to induce phosphorylation

and de-phosphorylation of transcriptional regulators of mitogenic agents such as cytokines, environmental stresses, hormones and growth factors.

The sensitivity of MAPKs to ROS generation has been noted, as the altering of the cellular redox state can trigger activation, particularly of JNK and p38, which are commonly referred to as stress kinases. ERK is predominantly linked to regulating cell proliferation (Yang, *et al.* 2003).

Owing to its central enzymatic activity in modulating cell proliferation, MAPKs represent a key target for FB_1. TNF-α signal transduction is known to be mediated by MAPKs, thus being responsible for inducing either cell proliferation or cell death. JNK is linked specifically to TNF-α-induced apoptosis, as it is activated by apoptosis signal regulating kinase 1 (ASK1). Both ASK1 and JNK are inhibited by glutathione-S-transferase (GST), yet this inhibition can be reversed by FB_1-induced oxidative stress, which is thought to be the underlying mechanism behind the ability of FB_1 to promote cell proliferation (Wattenberg, *et al.* 1996).

The observed occurrence of reactive species generation during TNF-α signalling, predominantly in the mitochondria, is indicative of its role in TNF-α-induced apoptosis. Consequences of reactive species production appear to include changes to the mitochondrial permeability transition (MPT), as well as mitochondrial swelling, however little is known about the underlying mechanism.

Research conducted on the murine fibrosarcoma cell line (L929 cells) demonstrated a correlation between cytotoxicity and TNF-induced ROS generation, which was presumed to be produced in the mitochondria and scavenged by the GSH system.

Several studies have provided evidence of the link between FB_1 and cytokine expression.

Elevated levels of TNF-α was observed in mouse liver and kidney cells treated with FB_1 (Bhandari and Sharma, 2002). Both FB_1 treated peritoneal mice macrophages and J774A

mouse macrophage cell line showed increases in TNF-α expression (Dugyala, *et al.* 1998). In contrast, swine alveolar macrophages demonstrated a reduction in TNF-α expression upon FB_1 treatment (Liu, *et al.* 2002), thus indicating a cell and tissue type-dependent response of FB_1 on cytokine expression.

Nitric oxide is a highly reactive molecule involved in regulatory processes in a range of biological events (Choi, *et al.* 2002), and its low-level regulation is necessary for the maintenance of cell homeostasis. Its role in regulating apoptosis and cell proliferation incorporates MAPK activation, as NO induces the gradual elevation of Ca^{2+} ions activating ERKs, which in turn stimulates cell division and hence proliferation. In a similar fashion, NO-induced activation of stress kinases p38 and JNK promote apoptosis. This occurs via the mitochondrial pathway, when cytochrome c is released from the mitochondria into the cytosol, leading towards caspase-3 activation, the executioner caspase (Choi, *et al.* 2002).

Thus inhibiting iNOS by blocking MAPK signalling molecules can considerably impact on the cellular homeostasis modulated by both iNOS and NO.

1.4 APOPTOSIS

Apoptosis is now known to be a specific form of cell death, of which there are several others. Apoptosis is a normal occurrence during the growth and degeneration of living organisms, and contributes maintaining cellular homeostasis. It also acts as a mode of defence during pathogenic invasion of a host organism, or upon cell damage (Rastogi, *et al.* 2009).

Apoptosis is triggered by a range of stimuli, and regulated via signal transduction as a result of cell signalling molecules such as TNF-α and MAPKs.

The morphological pathway of apoptosis clearly distinguishes it from other types of cell death. This pathway includes cell shrinkage, chromatin condensation or *pyknosis*, and the disintegration of the cell cytoskeleton, which causes bulges in the plasma membrane otherwise known as *blebbing*. This is followed by nuclear DNA fragmentation or *karyorrhexis*, and the formation of apoptotic bodies. These apoptotic bodies express cell surface markers such as phosphatidylserine, which allows phagocytic recognition whilst minimising the damage to surrounding tissue. Recombinant protein Annexin V binds to phosphatidylserine residues on apoptotic bodies, and is currently applied as an apoptotic detector (Elmore, 2007).

The induction of apoptosis occurs via the activation of a particular group of cysteine proteases, referred to as ~~"c~~aspases", which is incorporated into a cascade of pathway activations initiated by apoptotic stimuli, leading to the ~~"p~~rogrammed" death of the cell. Caspases are initially synthesized as inactive precursors, which undergo a proteolytic processing process prior to activation. A total of fourteen caspases have thus far been identified in mammals, and of this only a subset has been identified as directly functional in apoptotic regulation (Slee, 2000).

Inducing apoptosis is generally dependent on the nature of the stimuli and the pathway it initiates. This determines which caspases are expressed. Caspases initially present themselves in cells as an inactive proenzyme called a *procaspase*, which upon activation, initiates a cascade of procaspase activation. The ensued proteolytic cascade then amplifies the pathway associated with the activated procaspases, and heads toward ultimate apoptosis (Elmore, 2007).

Caspases are categorised in two general subsets. Upstream or apical caspases are aggregated upon receipt of apoptotic stimuli, and initiate a caspase cascade. Within this subset are caspase-2, -8, -9, -10, all having long N-terminal regions (prodomains) with motifs (caspase

recruitment domains (CARDs), and death effector domains (DEDs). Downstream, or executioner, caspases (caspase-3, -6, -7), are directly involved in cell destruction. These caspases have either prodomains or none at all (Slee 2000).

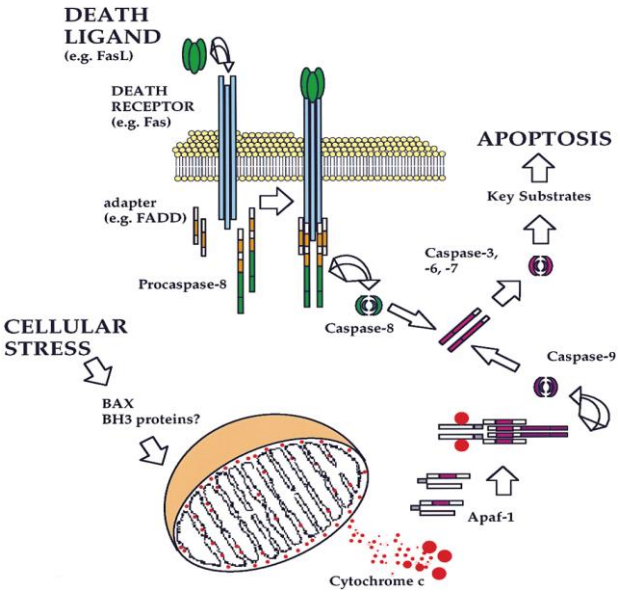

Figure 1.5: Pathways to caspase activation and apoptosis (Green, *et al.* 1998).

The known apoptotic pathways are the *intrinsic* or mitochondrial pathway, which depends on caspase-9; the *extrinsic* or death receptor pathway, which depends on caspase-2, -8, and -10; and the perforin/granzyme induced pathway, which is caspase-independent. All three pathways are said to merge at a single point called the *execution pathway*, marked by the activation of caspase 3, 6 and 7, resulting in apoptosis and the morphological characteristics as previously described (Elmore, 2007). These apoptotic pathways have long been thought to be energy- dependent and must therefore occur via a mitochondrial-dependent pathway. However, apoptotic characteristics such as externalisation of PS and membrane blebbing have been observed in mature erythrocytes that lack both mitochondria and nuclei. Erythrocytes are known to possess caspase activity, proposed to be induced in oxidative-stressed mature cells (Debabrata, *et al.* 2005).

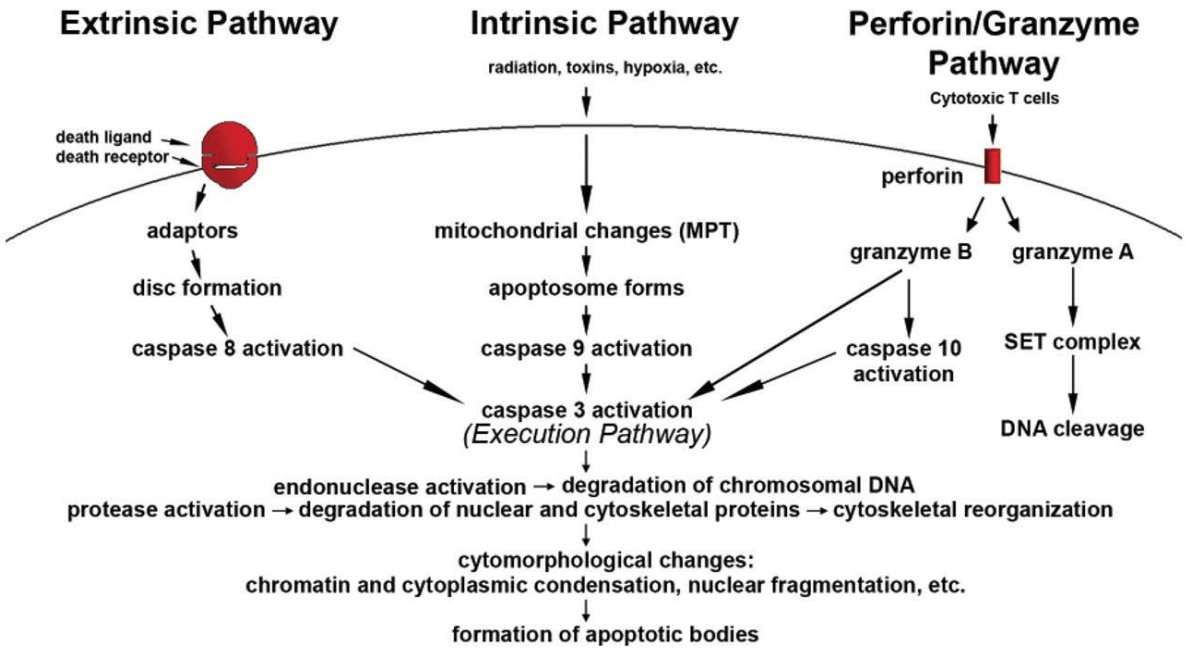

Figure 1.6: A Schematic representation of apoptosis, showing the key pathways (Elmore, 2007).

The intrinsic or mitochondrial pathway is induced by intracellular stress, and, DNA and endoplasmic reticulum (ER) damage. The intrinsic pathway is initiated by a range of stimuli, producing intracellular signals to either promote or inhibit apoptosis. For example, when insufficient cytokines are expressed, death programmes are not suppressed, and apoptosis is induced, whereas the presence of stimuli such as free radicals can initiate this suppression, thus inhibiting apoptosis (Elmore, 2007).

As the name suggests, mitochondrial permeabilization is an important stage in the intrinsic pathway. The opening of the mitochondrial permeability transition (MPT) pore and loss of mitochondrial membrane potential (MMP) is generally coordinated by fluctuated levels of apoptotic regulator Bcl-2, upon DNA damage. This is followed by the release of pro-apoptotic proteins cytochrome c, Smac/DIABLO and serine protease HtrA2/Omi from the intermembrane space into the cytosol. Smac/DIABLO and HtrA2/Omi both function by

blocking the activity of the inhibitors of apoptosis proteins (IAP) (Schimmer, 2004). A complex called an *apoptosome* subsequently forms when cytochrome c binds to apoptotic protease activating factor (Apaf-1) and procaspase-9 (Hill, *et al.* 2004). This stimulates caspase-9 activation. Additional proteins including Apoptosis Inducing Factor (AIF) and Endonuclease G (Endo G) are also released from the mitochondria but stimulate DNA fragmentation and pyknosis via a caspase-independent pathway (Rastogi, *et al.* 2009).

The Extrinsic pathway triggers apoptosis via interaction between receptors belonging to the TNF receptor gene superfamily and the appropriate ligand (Locksley, *et al.* 2001). Members of this family commonly possess an 80 amino acid long ~~"d~~eath domain" located on the cell surface, which is responsible for transmitting death signals to the intracellular signalling pathways. The TNF-α/TNFR1 or TNFR2 ligand-receptor bond in activated T cells is an example of this extrinsic pathway. Once the bond is formed, cytoplasmic adaptor proteins are recruited and attach to the receptor. In the case of the TNF ligand - TNF receptor bond, the adapter protein (TNF-Receptor Death Domain) TRADD is recruited. The death effector domain then undergoes dimerization as TRADD binds to procapase-8, forming the death inducing signal complex (DISC). The DISC can also be formed via the binding of the Fas ligand to the Fas receptor, which recruits the adaptor protein (Fas-associated Death Domain (FADD) in a similar fashion (Honglin, *et al.* 1998). This results in the auto-catalytic activation of procaspase-8 to form caspase-8, which in turn triggers apoptosis. At this point the intrinsic pathway can become involved, provided caspase-8 activation causes indirect activation of downstream caspases, BH3 interacting domain death agonist (Bid) cleavage. Fas-signalling is meant to occur via two pathways, both of which has been proposed to lead to mitochondrial damage. The Bcl2 family of proteins contains Bcl2 homology domains BH1,

BH2, BH3, and BH4, which are said to contribute to the anti-apoptotic characteristics of the Bcl2 family, particularly in the prevention of apoptosis-induced mitochondrial damage. These proteins may be able to disrupt the action of only the type II Fas-signalling pathway, but not type I (Honglin, *et al.* 1998).

The perforin/granzyme pathway involves the release of perforin/granzyme-A or B by cytotoxic T lymphocytes and NK cells (Martinvalet, *et al.* 2005). The resulting cytotoxicity occurs as the transmembrane pore-forming molecule perforin is secreted, followed by the release of cytoplasmic granules through the pore and into the target cell (Trapani and Smyth, 2002).

Granzyme B activates procaspase-10 owing to its ability to cleave proteins at aspartate residues. This cleaving ability also allows granzyme B to cleave Bid protein and induce the release of cytochrome c, which utilizes the mitochondrial pathway for the amplification of the death signal. In addition, granzyme B is involved in the direct activation of caspase-3, thus allowing the execution phase to occur without the involvement of signalling pathways (Barry and Bleackley, 2002).

The action of granzyme A occurs via its stimulation of DNA nicking, an important feature in apoptosis induction against tumour cells. This is achieved by the tumour suppressor gene product DNAse NM23-H1. The nucleosome assembly protein SET is cleaved from the SET complex and inhibits the NM23-H1 gene. The SET protein forms part of a complex that repairs DNA and chromatin structure, therefore as granzyme A cleaves this complex, DNA damage may appear, which may also contribute to apoptosis (Fan, *et al.* 2003).

1.5 OXIDATIVE STRESS

Oxidative stress has long been defined as an imbalance between oxidants and antioxidants, where an influx of free radicals is presented, without the necessary antioxidant response to act as scavengers. This definition predominantly but not exclusively refers to oxygen-derived free radicals or ROS, which are primarily generated at the mitochondrial respiratory chain as by-products of energy production and metabolism. Reactive species are involved in the regulation of a range of cellular functions including the activation of receptor and nuclear transcription factors, signal transduction and gene expression. For example, hydrogen peroxide (H_2O_2) activates NF-kB and Nrf2, along with other universal transcription factors (Packer, *et al.* 2007).

Reactive species are not however, limited to oxygen-derived radicals, as exemplified by free radicals NO and nitrogen monoxide (NO^+). The combination of NO with other free radical superoxides forms the potent non-radical oxidant peroxynitrite, which is widely known to induce tissue damage. Nitrogen monoxide participates in a range of physiological occurrences such as vasodilation and neuronal signalling and inflammation. It is synthesised by the enzyme nitric oxide synthase (NOS) and is present in various cell types (Packer, *et al.* 2007).

Due to the role of reactive species in signalling and control events via the altering of redox pathways, a new definition of oxidative stress was proposed as *"a disruption of redox signalling and control that recognizes the occurrence of compartmentalized cellular redox circuits"* (Jones, *et al.* 2006).

As mentioned earlier, the mitochondrial respiratory chain is cited as the main source for the synthesis of ROS, yet it is also the main target for their oxidative effects. As mitochondrial DNA (mtDNA) rests in close proximity to the respiratory chain, it is particularly vulnerable

to oxidative damage. An apoptotic pathway is triggered as a result of electron transport interruption, mitochondrial membrane depolarisation, and the inhibition of ATP synthesis (Ott, *et al.* 2007).

The iron-sulphur protein aconitase is found in the mitochondria, and is elemental in the Krebs cycle, being the enzyme involved in citrate to isocitrate conversion. Reactive species such as O^{-2-} directly oxidises and inactivates aconitases, resulting in iron release. Thus, the inevitable disruption of the Krebs cycle as a result of mitochondrial aconitase inhibition, impacts on energy production and cell viability (Farris, *et al.* 2005).

Glutathione (GSH) plays an important role in the mitochondrial antioxidant defence system. The mitochondria contains its own stock of GSH that controls the level of ROS within the cell via the action of GSH-linked enzymes Glutathione peroxidase 1 and 4 (Gpx1 and 4), which catalyses the reduction of radicals such as H_2O_2 (Schreck, *et al.* 1991). Although Gpx1 is the predominant isoform, Gpx4 was shown to be more efficient at reducing hydroperoxide groups on membrane phospholipids and lipoproteins, owing to its smaller size and larger hydrophobic surface, making it the main enzymatic mechanism against cellular membrane oxidative damage (Ott, *et al.* 2007).

Another important defence mechanism is the mitochondrial thioredoxin (Trx) system. Although Trx systems are present in the cytoplasm and nucleus, mitochondrial Trx operates independently, containing its own exclusive gene products Thioredoxin 2 (Trx2) and thioredoxin reductase 2 (TrxR2). Trx2 and TrxR2 function by potently reducing protein disulfides, the by-products of protein oxidation, as well as mixed disulfides between proteins and GSH (de/glutathionylation) (Ott, *et al.* 2007). This reduction mechanism is thought to assist with the protection of cysteine residues from modification by S-nitrosylation (Packer, *et al.* 2007).

Data has been presented that links TNF-α signalling with the oxidation of mitochondrial Trx2. Trx2 appears to play a distinct role in the regulation of TNF-α–induced ROS generation in the mitochondria, which in turn regulates processes such as apoptosis and cell proliferation via NF-κB activation.

As previously mentioned, the enzyme SMase has been implicated in TNFα-induced apoptosis. SMase is activated by TNF-α, which in turn hydrolyses SM, resulting in the production of ceramide, a known apoptotic regulator and inducer of oxidative stress (Cuzzocrea, *et al.* 2008). Liu *et al.* (1997) demonstrated in MCF7 human carcinoma cells that treatment with GSH inhibits the hydrolysis of SM by blocking the induction of neutral, magnesium dependent SMase (N-SMase) by TNF-α. However, when the same cell line was treated with TNF-α, a sharp decline in GSH levels was observed, and as a result, N-SMase was activated leading to SM hydrolysis and ceramide formation. This suggests that the effects of GSH are reversible and concentration dependent (Liu, *et al.* 1998).

Overproduction of ROS results in the depletion of GSH, which in turn affects an array of functions such as protein biosynthesis, immune function, and detoxification capacity (Ngondi, *et al.* 2006).

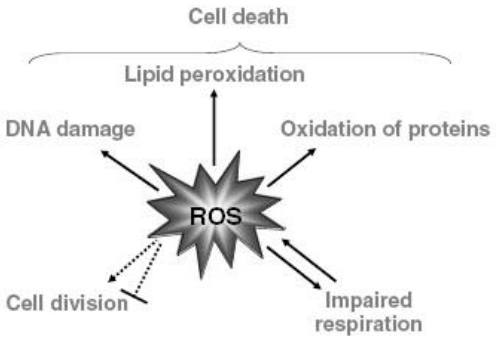

Figure 1.7: Effects of ROS on cellular functions and the induction of cell death - ROS induce DNA damage, oxidation of proteins, impair mitochondrial respiration, and dose-dependently either stimulate or inhibit cellular proliferation (Ott, *et al.* 2007).

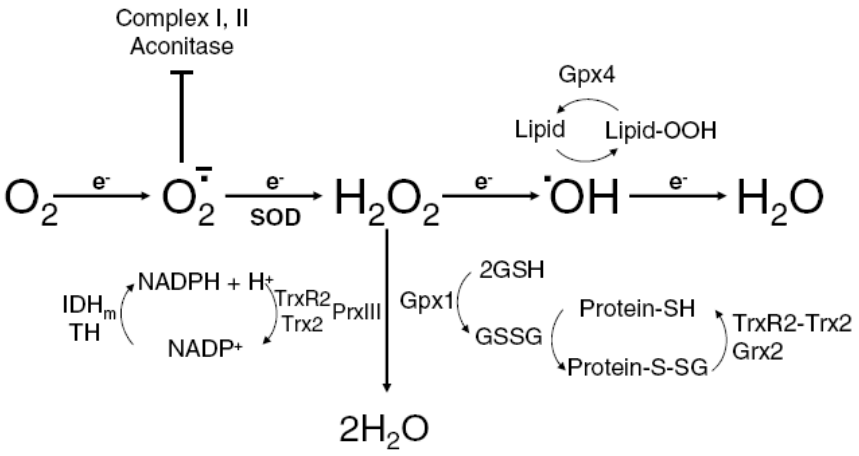

Figure 1.8: Formation, effects and inactivation of ROS in mitochondria (Ott, *et al.* 2007).

Lipid peroxidation predominantly acts on cellular membrane lipids. This results in membrane permeability, loss of membrane function, and the destabilising of membrane-bound receptors and enzymes (Abel, *et al.* 1998). By-products of lipid peroxidation are proposed to contribute to major health risks such as atherosclerosis, as oxidized lipids have been identified in human patients classified as high-risk for such lifestyle-related diseases. These by-products also induce redox-related cell signalling, which integrate with other signalling pathways to control cellular responses to extracellular stimuli.

In addition, lipid peroxidation impacts on mitochondrial functions such as maintenance of mitochondrial membrane potential (ψ), respiration and oxidative phosphorylation, mitochondrial Ca^{2+} buffering capacity and inner membrane barrier properties (Halliwell, *et al.* 1993).

CHAPTER 2

METABOLIC ACTIVITY OF JURKAT CELLS AFTER TREATMENT BY MTT ASSAY

2.1 MTT ASSAY

Abnormal cell metabolism, including energy and redox potential, are distinct characteristics of carcinogenicity. In order to maintain cell viability, a homeostatic relationship must exist among the growth requirements of the cell, the rate of production and energy use, and redox metabolites, without having to alter the levels of metabolic intermediates associated with other cell processes.

The methylthiazol tetrazolium (MTT) assay involves the reductive cleavage of the heterocyclic organic yellow salt 3-[4,5-dimethylthiazol-2-yl]-2,5-diphenyltetrazolium bromide, to the purple formazan product. The MTT assay is widely used for investigating cell proliferation and cytotoxicity. It is colorimetric, and formation of the purple formazan is indicative of cell viability, as only metabolically active cells are capable of converting MTT salt to formazan (Bernhard, *et al.* 2003).

Despite being used extensively in cell proliferation and cytotoxicity assays, the mechanism behind its bio-reductive properties remained elusive. It was initially proposed that MTT reduction was due to the succinate-dehydrogenase system via the mitochondrial respiratory chain. However, the ability of flavin oxidases and other non-mitochondrial dehydrogenases to

reduce MTT led to belief that an alternative mechanism was also involved. Berridge, *et al.* (1996) provided evidence of the involvement of reduced nicotimamide NADH and NADPH. Both NADH and NADPH are high-energy electron donors and their presence within the cell contributes to cellular homeostasis owing to their involvement in biosynthetic pathways. The primary association of NADPH is with cellular detoxification and the maintenance of the antioxidant defence system. An intermediate role in ATP synthesis and transcription repair in the nucleus is played by NADH. The oxidised NAD^+ is converted to $NADP^+$ via the action of NAD kinases. A functional role in cell signalling is played by $NADP^+$, as its conversion to secondary messengers during calcium signalling impacts on cellular processes (Agledal, *et al.* 2010).

2.2 Aims

The aim was to determine the cell viability of Jurkat cells treated with FB_1 and to calculate the concentration of FB_1 required to induce a 50% inhibition (IC_{50}) of live Jurkat cells.

2.3 Materials and Methods

2.3.1 Materials

Methylthiazol tetrazolium salt was purchased from Calbiochem (SA); dimethyl sulphoxide (DMSO) and PBS tablets were obtained from Merck (SA); 96 well microtitre plates were purchased from the Scientific Group (SA). All other chemicals were purchased from Merck (SA).

2.3.2 Jurkat cells

Jurkat cells are peripheral blood mononuclear cells that have been transformed to a continuous cell line via infection with Epstein - Barr virus (EBV). Jurkat cells originally derive from an acute T-cell leukaemia (ATCC TIB-152), and possess a pseudodiploid karyotype, due to spontaneously occurring chromosome and genetic abnormalities within the cell population (Neff and Reddy, 2008).

A cryovial of Jurkat cells was resuscitated by incubating at 37^{o}C for a few minutes. The cells were then suspended in 15 ml of pre-warmed culture medium (RPMI; 10% FCS; P/S), and centrifuged for 10 minutes and 400rpm at RT (eppendorf 5804 R). The supernatant was then discarded and the remaining pellet of cells re-suspended in 5 ml RPMI, and transferred to a tissue culture flask containing the appropriate amount of media. At approximately 80-90% confluency (1x10^{6} viable cell/ml), Jurkat cells were seeded into a 96-well microtitre plate (2.0×10^{4} cells/well), treated in triplicate with serial dilutions of FB_1 (0-500µM) made from a 1mg/ml stock (1384µM) at 37 ºC for 12h, 24 h and 48h.

2.3.3 Fumonisin B_1

A 1 in 10 dilution of 10mg/ml stock of FB_1 was prepared, having a final concentration of (1384µM). This was then serially diluted with deionised water, within the range of 0 - 500µM, and used in the subsequent assay. The derived IC_{50} value for FB_1 was used in all subsequent assays.

2.3.4 Methods

After the respective incubation period, MTT salt (5 mg/mL in PBS at pH 7.4) was added to the Jurkat cells and further incubated for 4 h at 37 ºC. These steps were performed in a safety

cabinet equipped with a vertical laminar flow hood, to ensure the protection of cell suspension from any foreign particles that may affect the experiment. The microtitre plate was then centrifuged (24^0C; 400g; 10 min) and the supernatants aspirated. Dimethyl sulphoxide (DMSO) (100 µL/well) was added to the wells and left to incubate for 1h. As a polar aprotic solvent, DMSO is unable to donate hydrogen, and is capable of dissolving both polar and non polar compounds. Hence DMSO solubilises the insoluble formazan formed. The optical density was measured at 570/690 nm, using a spectrophotometric plate reader (Bio-Tek µQuant).

Calculations

The assay was performed in triplicate and the mean cell viability was calculated by comparing the absorbance of each treatment to that of the control:

Cell Viability (%) = (Mean absorbance of treatment cells/Mean absorbance of control cells) x 100

Statistical Analysis

Based on MTT cell viability results, a FB_1 dose-response curve was plotted for each time period using GraphPad Prism v5.0 software (GraphPad Software Inc., La Jolla, USA), to determine the IC_{50} of FB_1 in Jurkat cells. The IC_{50} value obtained was used for Jurkat cell treatments in subsequent assays.

2.4 Results and Discussion

From the MTT data, the IC_{50} of live Jurkat cells after FB_1 treatment was determined (Figure 1.1).

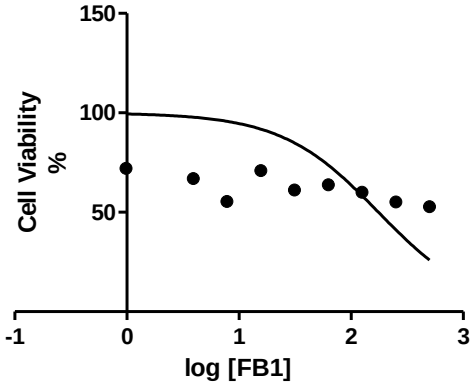

Figure 2.1: Nonlinear regression graph of log [FB_1] (µM) vs. cell viability in Jurkat cells. Serial dilution of FB_1 ranged from 0 to 500µM. IC_{50} value was extrapolated from the graph at a value of 175µM.

Using the nonlinear regression equation "log (inhibitor) vs. normalized response", the log of the FB_1 concentration was plotted against the cell viability after 48 h. The IC_{50} value was then extrapolated from the equation and a value of 175µM was obtained (Figure 1.1).

Maenetje, *et al.* (2008) investigated the cytotoxicity of known mycotoxins including FB_1 on human lymphocytes after 24 hours, and reported a dose-dependent decrease in cell viability as FB_1 concentration increased from 6.25 $x10^3$ parts per billion (ppb) to 25.0x 10^3 (ppb). In addition, a slight increase in cell viability was reported at a lower FB_1 concentration of 3.13 x 10^3 ppb. The authors attributed cytotoxicity to the ability of FB_1 to block the action of ceramide synthase, the enzyme responsible for sphingolipid metabolism, although the study

provided no data to conclude this. Owing to it lipophilic backbone, FB_1 bears strong structural similarity to the ceramide synthase-binding substrate sphinganine. The sphingoid base substrate converts to a sphingolipid product via the enzymatic action. As a result, FB_1 may be capable of inhibiting sphingolipid synthesis (Yin, *et al.* 1998). Sphingolipids are an important component of plasma membranes, and are associated with regulating signal transduction pathways such as cell proliferation and apoptosis (Luongo, *et al.* 2006). Therefore, the ability of FB_1 to block the synthesis of this regulatory molecule may result in uncontrolled cell proliferation, causing formation of the formazan product. This mechanism has been proposed for the carcinogenic properties of FB_1. An additional mechanism for cell cytotoxicity is the ability of FB_1 to promote oxidative stress. The iron-sulphur protein aconitase is found in the mitochondria, and is elemental in the Krebs cycle, being the enzyme involved in citrate-to-isocitrate conversion. Reactive species directly oxidise and inactivate aconitases, resulting in iron release. Thus, the inevitable disruption of the Krebs cycle as a result of mitochondrial aconitase inhibition, impacts on energy production and cell viability (Farris, *et al.* 2005).

Calculation of the IC_{50} value was first attempted in FB_1 -treated Jurkat cells at 12 and 24 h, using a serial dilution of FB_1 ranging from 0 to 500μM, however, exponential cell proliferation was observed at both time periods (data not shown). This indicated that cells were metabolically viable, and at very least FB_1 did not inhibit proliferation. Proliferation did however appear time-dependent, as cytotoxicity was observed after 48 h treatment. Despite small fluctuations, cell viability decreased with increasing concentrations of FB_1 (See Table 1.1).

Table 2.1 – Cell viability of Jurkat cells after 48h with FB_1 Concentration ([FB_1]) range from 0-500µM

[FB_1] (µM)	Viability (%)
500	52.8
250	55.2
125	60.1
62.5	63.8
31.25	61.2
15.63	70.9
7.81	55.5
3.91	66.9
0.98	72.1
0	100

CHAPTER 3

FLOW CYTOMETRIC ANALYSIS OF MITOCHONDRIAL MEMBRANE POTENTIAL AND APOPTOSIS OF FUMONISIN B_1 AND *SUTHERLANDIA FRUTESCENS*-TREATED JURKAT CELLS

3.1 Introduction

Apoptosis is a normal occurrence during the growth and degeneration of living organisms, and contributes to maintaining cellular homeostasis. It also acts as a mode of defence during pathogenic invasion of host organisms, or upon cell damage. Apoptosis is triggered by a range of stimuli, and regulated via signal transduction as a result of cell signalling molecules such as TNF-α (Rastogi, *et al.* 2009).

The key role of mitochondria in a cell is ATP generation via oxidative phosphorylation and oxygen consumption. The mitochondrion possesses a large, impermeable inner membrane containing enzymes responsible for oxidative phosphorylation. In addition to ATP generation, mitochondria also take part in the execution of apoptosis. Apoptotic cells undergo both extrinsic (receptor-mediated) and intrinsic (mitochondrial-mediated) signalling pathways, and both have been shown to recruit the mitochondrial death machinery, which amplifies the apoptotic response (Farris, *et al.* 2005).

The loss of mitochondrial membrane potential (MMP) and opening of the mitochondrial permeability transition (MPT) pore is associated with the intrinsic pathway towards apoptosis. This involves the release of apoptotic protein cytochrome c, which inevitably results in caspase-9 activation and mitochondrial depolarisation (Rastogi, *et al.* 2009) (See Literature Review). Hence mitochondria have generally been assessed for the determination of cell viability.

3.2 Flow Cytometry

Flow cytometry provides a mechanism by which cell populations can be distinguished via measurable markers; whether size, fluorescent stain, or *granular content* (the number of granules/other organelles contained within the cell). It involves the utilisation of laser light scattering and fluorescent emission to collect information from the sample being analysed. Flow cytometry finds predominant use in molecular biology laboratories for data extraction in clinical diagnostic procedures, such as immunophenotyping for diagnosis of acute and chronic leukaemias, immune-deficiencies (HIV) and lymphomas.

3.2.1 Continuous Flow

The cell samples are loaded into the central channel of the fluidics system, which is enclosed by an outer sheath containing continuously flowing fluid. As this fluid moves, the sample becomes constricted as the diameter of the central channel reduces. The sample then passes through the nozzle of the cytometer one particle at a time. This is referred to as *hydrodynamic focusing*, which limits the occurrence of nozzle blockage, as blockage prevents the analysis of individual particles. The high thermal capacity of the water safeguards the cells from damage by the laser beam (Ormerod, 2000).

3.2.2 Light

Subsequent to hydrodynamic focusing, the sample is exposed to beams of laser light. This is the stage where sample information is obtained. Generally, light in the flow cytometer is sourced from an argon ion laser, although arc lamps provide a cheaper but less effective option. The laser produces an oval-shaped light beam of a single wavelength at 488nm, aimed

directly at the buffer stream. The sample passes through the laser beam one particle at a time. Each particle to connect with the laser beam scatters light in all directions, and this scattered light is collected and measured by detector systems (Ormerod, 2000).

3.2.3 Fluorescence

If the samples are labelled with fluorochromes (fluorescent dyes used in biological system detection), upon exposure to the laser beams these fluorochromes become excited and the electrical impulse generated is analysed by computer software. Two commonly used fluorochrome labels are fluorescein isothiocyanate (FITC) and R-phycoerythrin (RPE), which are easily distinguished from each other as they are excited at different wavelengths (approx 488nm and 575nm respectively) (Ormerod, 2000).

3.2.4 Detection

The Forward Scatter Channel (FSC) collects light scattered through a small angle (approx 20^0 from the laser beam axis), in the forward direction. This enables particles to be sorted according to their size, which in the case of cells, helps to differentiate between living and dead cells, as live cells produce a larger degree of low-angle light scatter compared to dead cells (Ormerod 2000). The Side Scatter Channel (SSC) measures the light scattered at an approximately 90^0 angle from the laser beam axis. In cell samples, cells with a larger granular content scatter more light than other cells; thus the SSC sorts the sample according to this marker. The data collected is analysed and the information is often displayed as a histogram with the various parameters plotted against each other. For example, cell size can be plotted against cell fluorescence. A dot plot or contour plot allows multiple parameters to be displayed at the same time. In order to begin conducting analyses on the flow cytometer, the outer sheath must be filled and the waste tank emptied. The vacuum trap must also be cleared

of any water. After switching on the machine, the required protocol is selected according to the type of analysis being conducted (Ormerod, 2000).

3.3 JC-1 Assay

The cationic, lipophilic dye 5,5',6,6'-tetrachloro-1,1',3,3' tetraethylbenzimidazolyl-carbocyanine iodide or JC-1 is applied to measure the extent of mitochondrial membrane depolarisation. Cells with low levels of depolarisation possess a negatively charged membrane potential, which allows the positively charged JC-1 to enter and accumulate within the mitochondrial matrix. J-aggregates form when high concentrations of JC-1 dye is reached, resulting in considerable shifts in absorption and fluorescence maxima of the dye and the mitochondrial becoming fluorescent red (Smiley, *et al.* 1991).

JC-1 exists in a liquid crystal form and possesses a unique feature in its ability to rapidly form at desirable sites, and its display of ~~r~~esonance fluorescence". The large dye molecules allow them to diffuse slowly enough for their application as reporter molecules for localized biochemical events (Legrand, *et al.* 2001; Smiley, *et al.* 1991).

In depolarised cells however, the mitochondrial membrane potential does not remain intact, hence the JC-1 dye is unable to accumulate within the mitochondria. JC-1 thus remains in the cytoplasm and the cell appears fluorescent green. JC-1 has an absorption and fluorescence maximum of 585 nm for J-aggregates. It is relatively non-toxic and soluble, and is detected via flow cytometry.

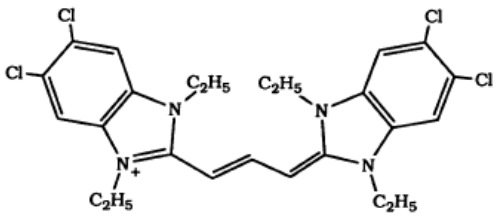

Figure 3.1: Structure of 5,5',6,6'-tetrachloro-1,1',3,3'-tetraethylbenzimidazolocarbocyanine iodide (JC-1) (Smiley, *et al.* 1991).

The JC-1 assay is a qualitative and quantitative cytofluorimetric method that allows cell populations with different mitochondria content to be identified. Its predominant use however, is in the investigations into the behaviour of mitochondria during a range of biological processes, most notably apoptosis (Salvioli, *et al.* 1997).

3.3.1 Aims

The aim was to assess the mitochondrial membrane potential of Jurkat cells treated with IC_{50} values of FB_1 and SF using the JC-1 assay.

3.3.2 Materials and Methods

3.3.2.1 Materials

The JC-1 Mitoscreen reagent was purchased from BD Biosciences (San Jose, CA). All additional reagents were purchased from Merck (SA).

3.3.2.2 Jurkat Cells

Jurkat cells were resuscitated, re-suspended and transferred to a tissue culture flask, as described in Chapter 2. At approximately 80-90% confluency ($1x10^6$ viable cell/ml), Jurkat cells were seeded into 4 x 15 ml Sterilin® tubes containing 5.0×10^4 cells/tube, and treated with IC_{50} values of FB_1 and SF. This procedure was conducted for all subsequent assays.

Table 3.1 – Treatment regime for Jurkat cells

Jurkat Cells	Treatment
Sample 1	FB_1 only
Sample 2	SF only
Sample 3	FB_1 and SF
Sample 4	Control (dH_20)

.

3.3.2.3 Sutherlandia frutescens (SF)

The stock solution of SF was calculated at 136.36mg/ml, and prepared via polar solvent extraction, as discussed in Appendix A. The prepared solution was used in all subsequent assays.

3.3.2.4 Methods

Sample Preparation

JC-1 working solution (100 µL) was added to 5×10^4 pre-treated Jurkat cells (See Table 3.1) in polystyrene cytometry tubes and vortexed thoroughly to remove any cell-to-cell clumping. Tubes were then incubated for 10 min at room temperature. Cells were washed in JC-1 wash buffer (1×), re-suspended in 200 µL flow cytometry sheath fluid and the tubes were gently shaken and placed into the flow cytometer.

Sample Instrumentation

Flow cytometry data from stained cells was obtained using a FACS Calibur (BD Biosciences) flow cytometer with CellQuest PRO v4.02 software (BD Biosciences). Cells were gated to exclude debris using FlowJo v7.1 software (Tree Star Inc., Ashland, USA) and expressed as a percentage of cells containing depolarised mitochondria.

Data analysis

Analysis of all samples was carried out using scatter/density plots and conducted using an excitation wavelength of 488nm. JC-1 monomers were detected at 527nm and JC-1 aggregates at 590nm. The total cell population was distinguished from the heterogeneous population and debris using forward and side scatter parameters of the Jurkat profile. Cells were gated in both the FL-1 and FL-2 channels, where JC-1 monomers and aggregates show fluorescence, and were recognised as having either polarised or depolarised mitochondria. FL-1 bright and FL-2 bright were indicative of healthy, polarised cells, while a decrease in the FL-2 channel when the FL-1 remains high indicated cells with mitochondrial depolarisation.

Statistical Analysis

Flow cytometric data was analysed using GraphPad Prism v5.0 software (GraphPad Software Inc., La Jolla, USA). Statistical significance between among treatments was determined using One-Way Analysis of Variance (ANOVA) and the Bonferroni post test. A probability value (p) of less than 0.05 ($p<0.05$) was considered statistically significant. This technique was applied to data from all subsequent assays.

3.3.3 Results and Discussion

The JC-1 assay measures mitochondrial depolarisation, which is an indicator of apoptosis. Results for the JC-1 assay are expressed as the percentage of cells containing depolarised mitochondria. The highest depolarization value was in SF-treated cells (18.5%), showing no significance when compared to all other treatments. A value of 12.3% was seen for FB_1 and the combination treatment stood at 12.2% (See Figure 3.3). Both values showed no significance when compared to all other treatments. The control treatment value was 13.5%.

Mitochondrial membrane potential is influenced not only by mitochondrial activity, but also by the overall energised state of the cell, including oxygen consumption, NADH:NAD^+ ratio, and cytosolic ATP production (Sternfeld, *et al.* 2009). Thus, the reported depolarisation in the control treatment may be a result of the complex nature of Jurkat cells, as they are a transformed cell line and have higher energy requirements. This indicates that MMP may not be the most suitable primary apoptotic marker, rather an indicator of the energetic state of the cell. In a study investigating MMP in blood mononuclear cells from HIV-1 treatment naive patients, a decrease in MMP was observed despite no increase in apoptotic rate, which implies MMP may not be a definitive characteristic of apoptosis (Sternfeld, *et al.* 2009). The lack of significance in mitochondrial depolarisation left expectations for data from subsequent apoptotic assays.

Fumonisin B_1 has been proposed to increase molecular oxygen transport close to the surface of cell membranes (Yin et. al 1998). The mitochondrial respiratory chain has been cited as both the primary source for ROS synthesis, as well as the main target for their oxidative effects. A lack of oxygen results in the utilization of glycolysis-produced ATP by mitochondria in order to maintain MMP (Sternfeld, *et al.* 2009). Also, mitochondrial DNA (mtDNA) rests in close proximity to the respiratory chain, and as a result is particularly

vulnerable to oxidative damage. The triggering of an apoptotic pathway results from electron transport interruption, mitochondrial membrane depolarisation, and insufficient ATP (Fariss, *et al.* 2005; Ott, *et al.* 2007). FB_1 has been proposed to induce mitochondrial depolarisation via its ability to increase oxygen transport and stimulate reactive species (Stockmann-Juvala, 2004), which may explain the observed depolarisation in FB_1-treated cells, although no significance was observed when compared to the control treatment.

Gamma amino butyric acid (GABA) is a constituent of SF, which may be capable of altering mitochondrial polarity by disrupting the mitochondrial proton gradient, owing to its nature as a weak acid. GABA is capable of reducing intra-mitochondrial NAD+ to NADH; which in turn donates its electrons to the mitochondrial electron transport chain, thus altering MMP (Brand and Chappell, 1973). Additionally, the presence of GABA opens up the $GABA_A$ receptors, allowing an influx of chloride (Cl^-) ions, which affects membrane polarization (Ojewole, 2008). The data shows an increase in mitochondrial depolarisation in cells treated with SF alone, in which GABA may be a contributing factor.

The observed treatment value for cells treated in combination was almost level with cells treated with FB_1 only. This implies an antagonistic role for FB_1 against SF.

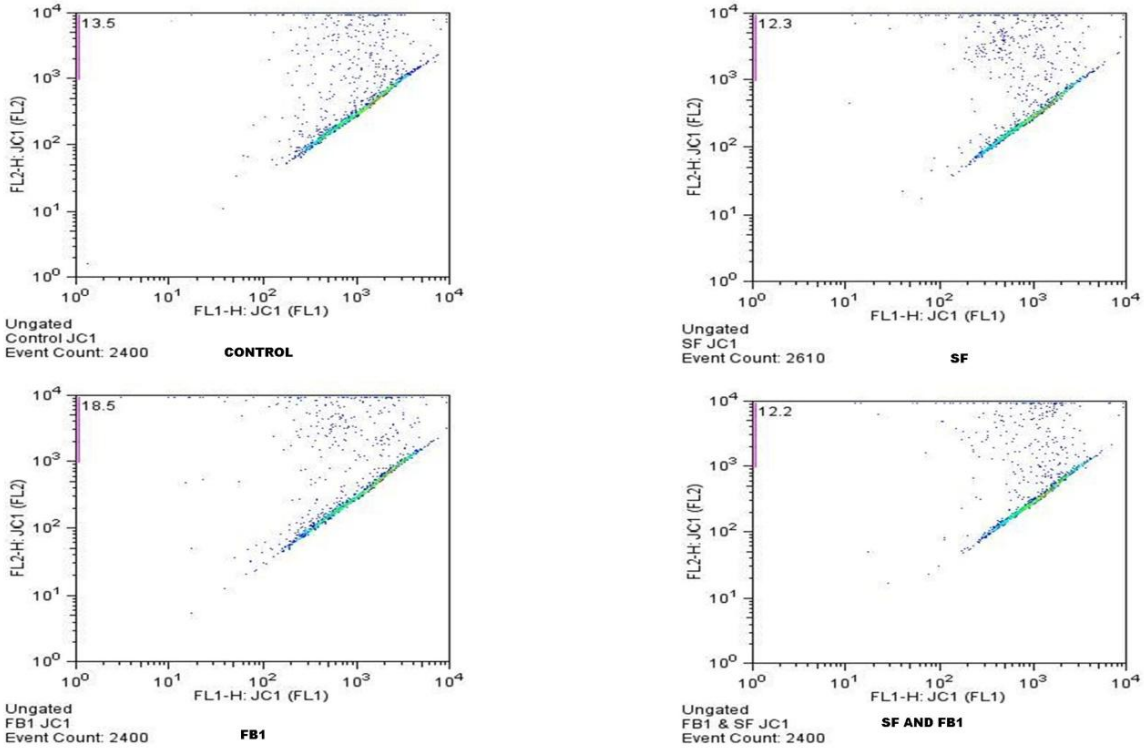

Figure 3.2 – JC-1 Flow Cytometry Scatter Plot Diagram

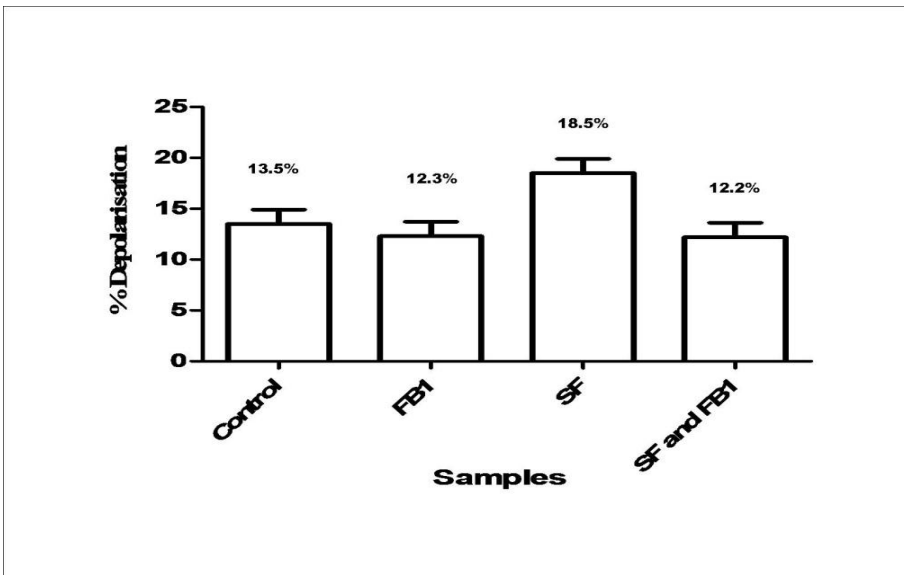

Figure 3.3 – JC-1 Assay results for treatment samples.

3.4 Annexin V Assay

The lipid phosphatidylserine (PS) has an important function in apoptosis. It is found on the surface of apoptotic cells as an ―eat me" signal for phagocyte/macrophage recognition. The positioning of PS on cell surfaces is dependent on caspase activation, hence its use as an indicator of caspase-dependent apoptosis (Crimmi and Esposti, 2010). Although receptors that bind to ligands other than PS and enable recognition exist, many of these ligands remain unknown (Fadok, *et al.* 2003). Phosphatidylserine does appear to be most significant, as it has been reported that apoptotic cells that did not express PS were not recognised by both mouse macrophages and HT-1080 cells (Fadok, *et al.* 2000).

The 35-kDa Ca^{2+} -binding recombinant protein Annexin V was developed as an apoptotic detector as it binds to PS residues on cells undergoing apoptosis. Biotinylated-annexin is used to label cells in all stages of apoptosis, allowing for detection by flow cytometry. A significant disadvantage of Annexin V is the fact that it can also attach to necrotic cells as well as apoptotic, thus limiting its specificity. This is overcome in flow cytometry detection by incorporating DNA binding dyes capable of distinguishing between necrosis and apoptosis (Huerta, *et al.* 2007).

3.4.1 Aims

The aim was to assess phosphatidylserine (PS) binding in Jurkat cells treated with IC_{50} values of FB_1 and SF using the Annexin V assay.

3.4.2 Material and Methods

3.4.2.1 Materials

Annexin-V-FLUOS staining kit was purchased from Roche Diagnostics (Penzberg, Germany). All other reagents were purchased from Merck (SA).

Annexin V-FLUOS labelling solution was prepared by diluting 20µl of the Annexin-V-FLUOS labelling reagent and 1ml of the propidium iodide (PI) incubation buffer.

3.4.2.2 Methods

Sample Preparation

An aliquot of 5 x 10^4 cells were transferred to eppendorf tubes and pelleted by centrifugation. Cells were then re-suspended in the Annexin-V-FLUOS labelling solution, incubated in the dark for 15 min and transferred to appropriately labelled polystyrene flow cytometric tubes.

Sample Instrumentation and Analysis

Annexin-V-FLUOS data were analysed using a FACS Calibur flow cytometer. Prior to analysis, 500µL of an incubation buffer was added to each sample and the tubes were lightly shaken and placed in the flow cytometer. Analysis of all samples was conducted using an excitation wavelength of 488nm. Subsequently, FL1 (Annexin-V-FITC-PS) and FL3 (propidium iodide-DNA) signals were detected via 515nm and 600nm bandpass filters respectively.

Data Analysis

Data was acquired with CellQuest PRO v4.0.2 software (BD Biosciences) and analyses using FlowJO v7.1 Software (Tree Star, Inc.) Analysis was carried out using scatter/density plots.

The total cell population was distinguished from the heterogeneous population and debris using forward and side scatter parameters of the Jurkat profile. Cells were gated in the respective fluorescent probes. The Jurkat population was gated at the 10^2 mark on the FL1 and FL3 channels creating cluster gates, thereby differentiating apoptotic and necrotic cells. Apoptotic cells were Annexin-V-FITC positive (x-axis) but PI negative (y-axis) (bottom right quadrant) and necrotic cells were positive for both Annexin-V-FITC and PI (top right quadrant)

Statistical Analysis

Statistical significance was determined using One-Way Analysis of Variance (ANOVA) and the Bonferroni post test on GraphPad Prism v5.0 software (GraphPad Software Inc., La Jolla, USA) A probability value (p) of less than 0.05 [$p<0.05$] was considered statistically significant.

3.4 Results and Discussion

Results for the Annexin V assay are expressed in percentage of PS externalisation (%). The combination treatment had the highest value of 29.1 %, showing no significance against the control value, but significant when compared to SF-treated cells [$p<0.05$]. A value of 24.3 % was seen for FB_1, which was significant when compared to SF [$p<0.05$], but not against the other treatments. The lowest value was observed for SF at 3.69 %, which was significant when compared to FB_1, combination treatment, and the control [$p<0.05$]. The control treatment value was 23.9 % (See Figure 3.5).

Although the Jurkat T cell line expresses similar markers as those found in normal T lymphocytes, proliferation occurs at a much faster rate, which may explain the results observed in the control cells.

The low value of Annexin binding in SF-treated cells was unexpected, and upon initial observation appears to represent an inhibition of apoptosis. The primary location for PS synthesis appears to be in mitochondria-associated membranes of the endoplasmic reticulum. There is no evidence to suggest that significant changes in mitochondrial PS levels occur during apoptosis, except in cases where oxidative stress is involved. Oxidation of PS by reactive species generated from the mitochondrial respiratory chain has been strongly linked to its externalization and role in the phagocytosis of apoptotic cells (Serenkan, *et al.* 2004). A likely mechanism behind this involves the electrostatic interaction of positively charged cytochrome c from the mitochondria with negatively charged PS, which catalyses PS oxidation (Serenkan, *et al.* 2004). Therefore, the low levels of Annexin V binding observed could be a result of the absence of PS oxidation in SF-treated cells. Reports have indicated that SF may possess antioxidant activity (Fernandes, *et al.* 2004), which may have inhibited PS oxidation and hence prevented its externalization. However it has also been demonstrated that although antioxidant activity may inhibit PS oxidation (Jiang, *et al.* 2003); it may not necessarily block phagocytosis or even prevent PS externalization. A study involving the treatment of Jurkat cells with potent antioxidant Vitamin E, showed no changes in PS externalization, phagocytosis or other apoptotic biomarkers, despite having no detectable levels of PS oxidation (Serenkan, *et al.* 2004). Although results for SF-treated cells did not correlate with JC-1 data, which indicates that some level of mitochondrial depolarisation occurred within SF-treated cells, as it was concluded that MMP is not a primary apoptotic marker, it may not be reflective of the true apoptotic state of the cell.

Cells treated in combination with both SF and FB_1 showed a marked reversal in PS binding, which may be indicative of increased PS oxidation via reactive species generated by FB_1, causing an increase in PS externalization.

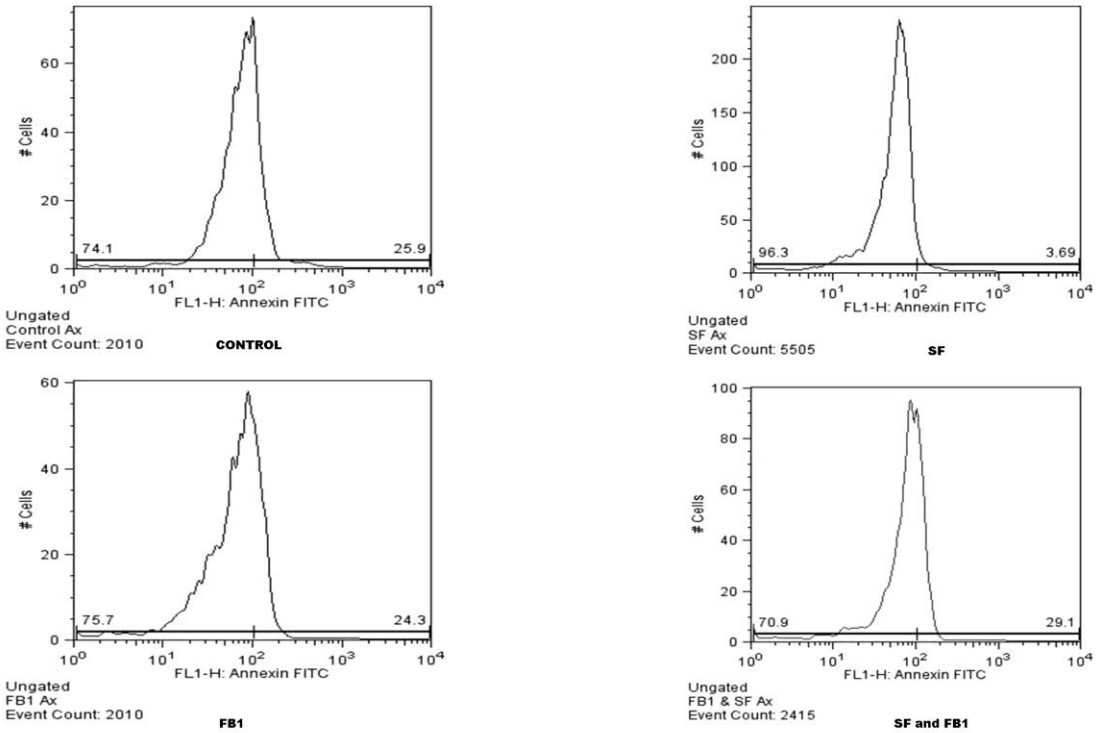

Figure 3.4 – Annexin V Flow Cytometry Scatter Plot Diagram

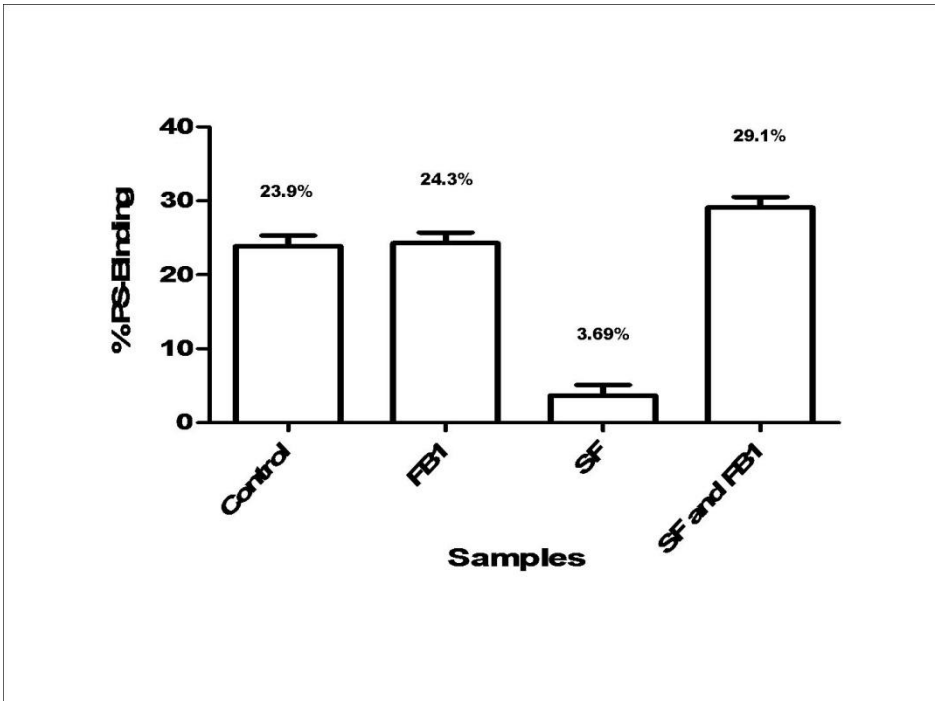

Figure 3.5 – Annexin V results for treatment samples.

CHAPTER 4

LUMINOMETRIC ANALYSIS OF FUMONISIN B_1- AND *SUTHERLANDIA FRUTESCENS* TREATED JURKAT CELLS

4.1 Caspase Assays

The induction of apoptosis occurs *via* the activation caspases, which are incorporated into a cascade of pathway activations initiated by apoptotic stimuli, leading to the ―programmed" death of the cell. Caspases are initially synthesized as inactive precursors, which prior to activation undergo proteolytic processing. In mammals, a total of fourteen caspases have been identified to date. Of these, only a subset has been linked with a direct function in apoptotic regulation (Slee, *et al.* 2000).

All three pathways involved in apoptosis (intrinsic, extrinsic and perforin/granzyme) are considered to merge at a single point called the *execution pathway*, which is defined by the activation of caspase 3, 6 and 7, resulting in the characteristic morphological changes seen in apoptosis (Elmore, 2007).

Apoptotic induction is generally dependent on the nature of the stimuli and the pathway it initiates. This will determine which caspases are expressed. Caspases initially present themselves in cells as an inactive proenzyme called a *procaspase*, which upon activation goes on to initiate a cascade of procaspase activation. This proteolytic cascade amplifies the pathway associated with the activated procaspases, ultimately leading to cell death.

Caspases belong to two general subsets. The upstream or apical caspases become aggregated upon receipt of apoptotic stimuli, and initiate a caspase cascade. Within this subset is caspase-2, -8, -9, -10, which have long N-terminal regions (prodomains) containing specific motifs – the caspase recruitment domains (CARDs), and death effector domains (DEDs).

Downstream, or executioner, caspases (caspase-3, -6, -7), are directly involved in cell destruction. These caspases may or may not possess prodomains (Slee, *et al.* 2000).

Caspase-Glo® Assays operate via a bioluminescent system, where a complex containing a luminogenic substrate and the enzyme luciferase is added to the cell sample. The substrate is then cleaved by the respective caspases, resulting in the generation of a luminescent signal, which is directly proportional to the level of caspase activity present in the cell (Karvinen, 2002).

4.1.1 Aims

The aim was to investigate caspase-3/7, -8 and -9 activities in FB_1 and SF-treated Jurkat cells using a luminometer.

4.1.2 Materials and Methods

4.1.2.1 Materials

Caspase activity was measured by the Caspase-Glo® assay.

[This involves the peptide-conjugated luminescent substrate Z-DEVD-aminoluciferin, which was combined to a stable recombinant firefly luciferase, Ultra-Glo™ Luciferase (Promega Corporation).] 10 μL of either Caspase-Glo® 3/7, 8 or 9 reagent (Promega) was added and allowed to react.

4.1.3.2 Method

Prior to analysis, Caspase-Glo® Reagents were prepared (see Appendix D) .The reagent was allowed to equilibrate to RT and thoroughly mixed. 2.0x 10^4 Jurkat cells re-suspended in PBS, pre-treated with SF and FB_1, and aliquotted into a white luminometer plate. 100μL of Caspase-Glo® 3/7, 8 or 9 Reagent was added to each well. The plate was gently mixed using a plate shaker at 300–500rpm for 30 seconds, and incubated at room temperature in the dark for 30 minutes. Following incubation, the luminescent signal produced by mono-oxygenation of amino-luciferin was measured with a microplate luminometer (Turner Biosystems, Sunnyvale, USA), and results expressed as Relative Light Units (RLU).

Statistical Analysis

Statistical significance was determined using One-Way Analysis of Variance (ANOVA) and the Bonferroni post test on GraphPad Prism v5.0 software (GraphPad Software Inc., La Jolla,

USA). A probability value (p) of less than 0.05 [$p<0.05$] was considered statistically significant.

4.1.3 Results and Discussion

Results for the caspase assays are expressed as Relative Light Units (RLU). For the caspase-3/7 assay, SF treated cells had the highest value of 86.79 RLU, which was not significant when compared to any of the other treatment data sets. Cells treated with FB_1 had a value of 14.35 RLU and also showed no significance compared to other treatment data sets. The combination treatment of FB_1 and SF was 6.61 RLU and again no significance was noted. The control treatment was measured at1.46 RLU (See Figure 4.1).

Values for Caspase-8 activation were highest in SF-treated cells at 40.10 RLU, and showed significance when compared to data sets of all other treatment samples [$p<0.05$]. FB_1 (11.43 RLU) showed significance when compared to SF [$p<0.05$], but not against control and combination treatments; combination treatment value was 21.42 RLU and was significant when compared to control and SF treatment, [$p<0.05$], but not against FB_1.The control treatment was measured at 1.28 RLU (See Figure 4.2).

In caspase-9 activation, the combination treatment had the highest value of 11.07 RLU, and was significant compared to FB_1 and control treatments [$p<0.05$]. SF treatment value was also significant against control and FB_1 treatments (9.92 RLU – [$p<0.05$]), but not against combination treatment. FB_1 had a value of 3.58 RLU, and showed significance against all treatments [$p<0.05$], while the control treatment value was measured at 0.28 RLU (See Figure 4.3).

Caspase-3 is recognised as the ―key-executioner caspase", as its activation leads to the irreversible progression of the apoptotic pathway, and it is primarily responsible for apoptosis-associated chromatin margination, DNA fragmentation, and nuclear collapse (O'Brien, *et al.* 2005). Caspase 3 activity was markedly higher in cells treated with SF alone, which may suggest that SF induces the execution pathways, leading to the irreversible progression towards apoptosis. The combination treatment value was lower than the SF treated cells, implying that FB_1 may antagonise the effect of SF on caspase-3 activation. This anti-apoptotic effect may possibly form part of its carcinogenic mechanism of promoting cell proliferation. However, the combination treatment was also lower than FB_1treated cells, which suggests an element of synergy may exist between SF and FB_1 that further inhibits apoptosis (See Figure 4.1). Results here did not correlate with Annexin data, and demonstrated that apoptosis did occur and was not inhibited in SF-treated cells as indicated by Annexin results.

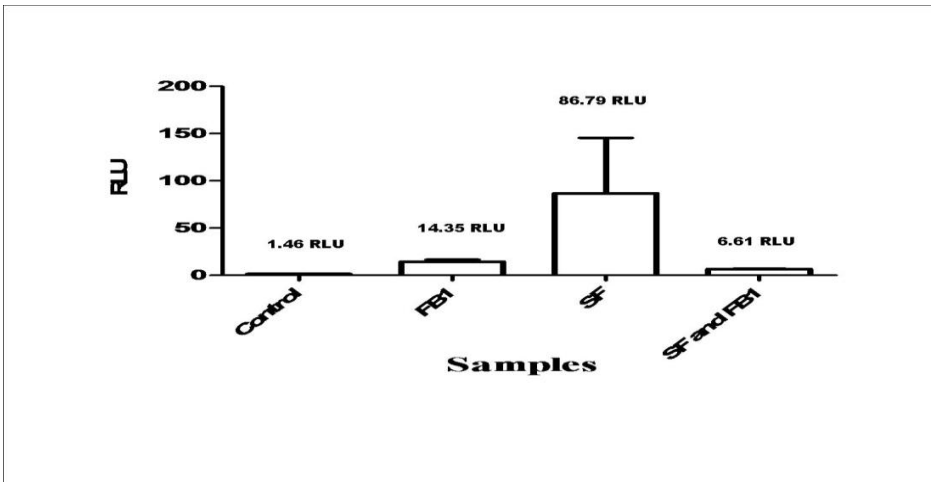

Figure 4.1 – Caspase-3 and -7 Assay results for treatment samples (RLU –Relative Light Units).

Caspase-8 plays a key role in the extrinsic pathway, or signalling-induced apoptosis (Honglin, *et al.* 1998). The extrinsic pathway triggers apoptosis via the interaction between receptors belonging to the TNF receptor gene superfamily and the appropriate ligand

(Locksley, *et al.* 2001). Activation of caspase-8 occurs via the signalling molecules Fas and TNF-α, and is thought to induce downstream apoptotic events such as caspase-3 activation and mitochondrial damage (Honglin, *et al.* 1998). However, caspase-8 and caspase-3 activation associated with oxidative stress and osmotic shock, have been observed in mature red cells that lack mitochondria (Debabrata, *et al.* 2005).

Caspase-8 activation was significantly higher in cells treated with SF alone compared to all other treatments (FB_1 alone, SF and FB_1 and control) [$p<0.05$]. This suggests that SF induces apoptosis via the death receptor-mediated extrinsic pathway. Results also indicate that FB_1 has an antagonistic effect on SF, as caspase-8 activation is significantly reduced (approximately 50%) in combination treatment. The combination treatment value was almost double the value in FB_1-treated cells however, indicating the positive action of SF in activating caspase-8 (See Figure 4.2).

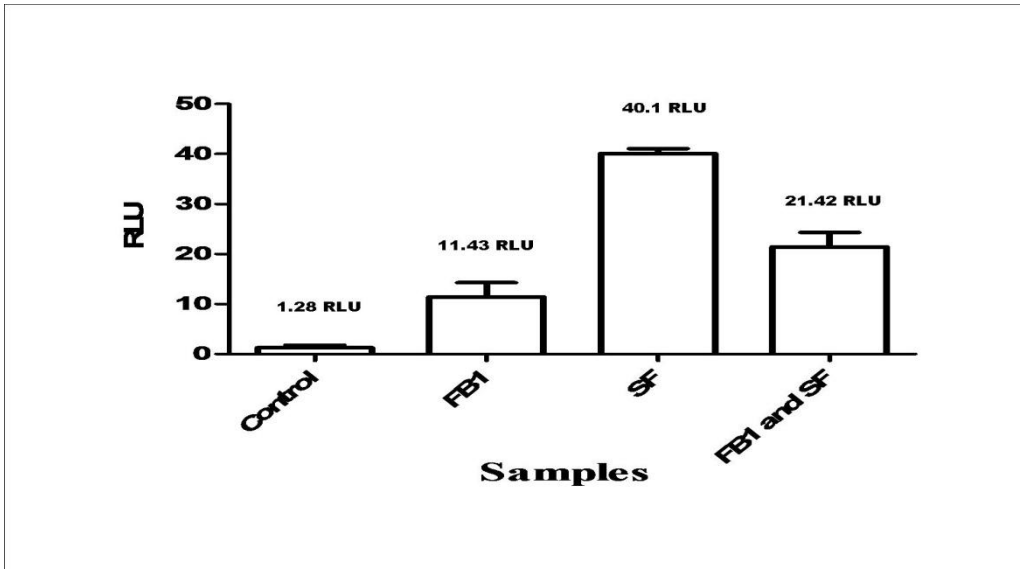

Figure 4.2 – Caspase-8 Assay results for treatment samples (RLU – Relative Light Units).

Caspase-9 activation is associated with the intrinsic or mitochondrial pathway, which is induced by intracellular stress and DNA and Endoplasmic Reticulum (ER) damage.

Cytochrome c associates with monomeric Apaf-1 upon its release from the mitochondria and entry into the cytosol and the subsequent conformational change promotes the oligomerization of Apaf-1, the recruitment of caspase-9, and the formation of the apoptosome complex. It is within this complex that caspase-9 has been observed to undergo rapid proteolytic maturation (Hill, *et al.* 2004).

Although caspase-9 was detected, its activation was not as prevalent when compared to caspase-3/7 and -8. Activation was higher in combination-treated cells compared to cells treated with SF alone, indicating that an FB_1-induced apoptotic pathway may be attributed to caspase-9 activation, as it was the only caspase to be synergistically activated by combination treatment. These results also suggest that the mitochondrial pathway may not be the primary mechanism involved in SF-induced apoptosis (See Figure 4.3).

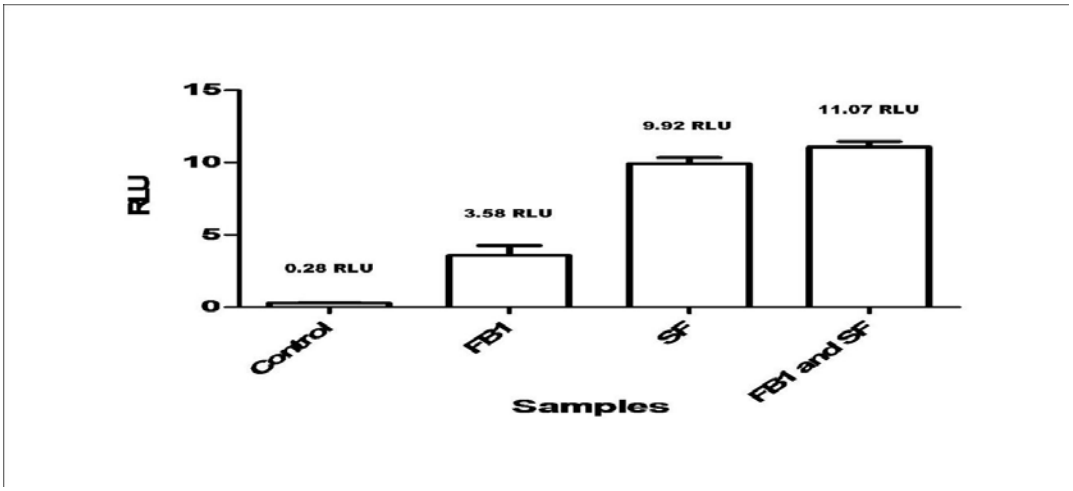

Figure 4.3 – Caspase-9 Assay results for treatment samples (RLU – Relative Light Units).

Table 4.1 – Caspase Assay Results

CASPASES	CONTROL (RLU)	FB_1 (RLU)	SF (RLU)	SF +FB_1 (RLU)
-3/-7	1.46	14.35	86.79	6.61
-8	1.28	11.43	40.1	21.42
-9	0.28	3.58	9.92	11.07

RLU – Relative Light Units)

4.2 Glutathione Luminometry Assay

The tripeptide GSH is a potent free radical scavenger, and acts by donating electrons to the enzyme glutathione peroxidase in order to facilitate the reduction of reactive species such as hydroperoxides. In addition to its antioxidant activity, nuclear GSH is associated with an increase in cell proliferation, although the precise mechanism remains unclear (Pallardo, *et al.* 2009). Depletion of GSH in the mitochondria is considered to be a common and early indirect marker of apoptosis, which occurs as a result of reactive species overproduction and DNA damage (Pallardo, *et al.* 2009).

Glutathione is quantified via the action of glutathione reductase. 5,5'-dithio-*bis*-2-nitrobenzoic acid (DTNB) reacts with the sulphydryl group of GSH to produce a yellow compound with 5-thio-2-nitrobenzoic acid (TNB). This mixed disulphide (GSTNB) is reduced by glutathione reductase causing the GSH to be reduced and more TNB to be produced. The concentration of GSH in the sample is directly proportional to the rate of TNB production, which is in turn directly proportional to the recycling reaction. Hence, measuring

the absorbance of TNB gives an accurate estimation of the GSH concentration present in the sample.

4.2.1 Aims

The aim was to measure the GSH antioxidant response in Jurkat cells treated with FB_1 and SF.

4.2.2 Materials and Methods

4.2.2.1 Materials

The GSH-Glo ™ Glutathione Assay was purchased from Promega, (Madison, USA). All other reagents were purchased from Merck (SA).

4.2.2.2 Method

Standards of GSH (0 μM – 5 μM) were prepared from a 5 mM stock solution, and added to the wells (50 μL) of the microtitre plate. 2x GSH-Glo ™ Reagent was prepared according to the manufacturer's instructions, added to each well, (50 μL/well), and incubated at RT for 30min. Reconstituted Luciferin Detection Reagent (100 μL) was added to each well and incubated for 15min. The luminescence was measured on a Modulus ™ microplate luminometer (Turner Biosystems, Sunnyvale, USA). A standard curve was derived using the GSH standards and the GSH concentration in each sample was extrapolated from the equation.

Statistical Analysis

Statistical significance was determined using One-Way Analysis of Variance (ANOVA) and the Bonferroni post test on GraphPad Prism v5.0 software (GraphPad Software Inc., La Jolla,

USA). A probability value (p) of less than 0.05 [$p<0.05$] was considered statistically significant.

4.2.3 Results and Discussion

Concentration values for GSH were determined by linear extrapolation from the standard curve and expressed in μM. Concentrations of GSH were lowest in FB_1-treated cells (0.3μM), and showed significance when compared to the control sample [$p<0.05$], but not against other treatments. SF-treated cells had a value of 0.48 μM, which was also significant when compared to the control treatment [$p<0.05$], and was slightly higher in value than FB_1, with no statistical significance. The combination treatment had a value of 0.94 μM, and was significant against the control value, [$p<0.05$], but not against the other treatments. The control treatment had a value of 2.79 μM (See Figure 4.4).

Glutathione plays an important role in the mitochondrial antioxidant defence system. The mitochondria contains its own stock of GSH that controls the level of reactive species within the cell via the action of GSH-linked enzymes Glutathione peroxidase 1 and 4 (Gpx1 and 4), which catalyses the reduction of radicals such as hydrogen peroxide (H_2O_2) (Schreck, *et al.* 1991). Overproduction of reactive species results in the GSH depletion, which in turn can affect an array of functions such as protein biosynthesis, immune function, and detoxification capacity (Ngondi, *et al.* 2006). Glucose transported into the cell undergoes phosphorylation to become glucose-6-phosphate (G6P), which is then oxidised in the pentose phosphate pathway (PPP) to produce NADPH. This is catalysed by the enzyme G6P dehydrogenase (G6PD). Not only is NADPH a key co-factor in fatty acid, nucleotide and amino acid biosynthesis; it also has an important role in cellular antioxidant activity, as it is responsible for the maintenance of GSH in a reduced state, which allows for the prevention of oxidative damage (Buchakjian and Kornbluth, 2010). Thus, the disruption of G6P oxidation by reactive

species generation may inhibit NADPH synthesis, and as a result reduce GSH levels. The weak acid nature of GABA may also contribute to GSH depletion via a disruption of the proton gradient associated with G6P oxidation.

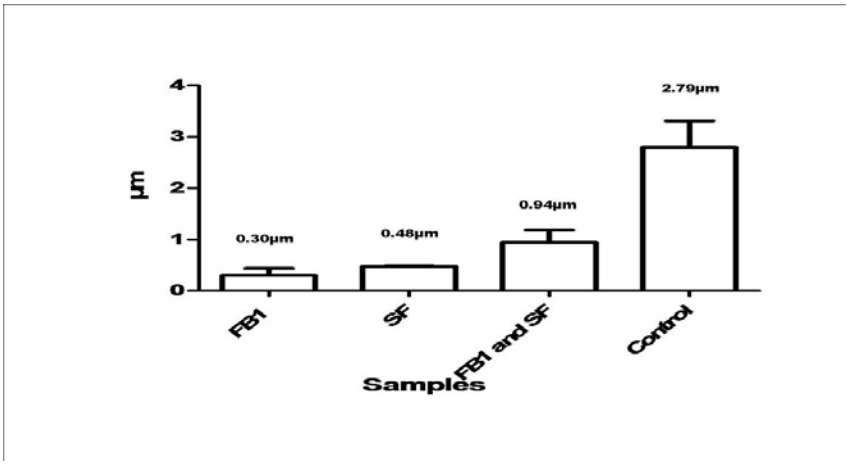

Figure 4.4 – Glutathione (GSH) Assay results for treatment samples.

In FB_1-treated cells, it is possible that FB_1 depleted GSH by inducing reactive species generation, resulting in subsequent oxidative damage. The GABA content of SF may have contributed to the observed GSH depletion in SF-treated cells. Based on the GSH concentration observed in combination treatment, it appeared that SF and FB_1 may play a synergistic role in maintaining/increasing GSH levels.

4.3 ATP Quantification

Adenosine triphosphate (ATP) has been described as the ―principal energy currency of the cell". ATP is recycled from adenosine diphosphate (ADP), during a process referred to as oxidative phosphorylation.

Generally, ATP synthesis occurs during respiratory electron transfer reactions in the mitochondria. Energy produced during these reactions is coupled to an electrochemical gradient of protons attached to the mitochondrial transmembrane, and used to drive the synthesis of ATP via the action of ATP synthase.

The ATP assay utilizes bioluminescence to quantify the presence of ATP in metabolically active cells, and hence provides useful information on cell viability or cytotoxicity.

The concentration of ATP is relatively uniform in each cell type, and is used as a marker for cell viability owing to the fact that its concentration rapidly declines in metabolically active cells undergoing apoptotic cell death. As a result, proliferation or cytotoxicity is expressed as a concentration-dependent increase or reduction in the bioluminescent measurement of ATP in cells subsequent to xenobiotic exposure. The principle of the bioluminescent ATP assay involves the use of luciferase enzyme, which catalyzes light formation from the reaction between ATP and the substrate luciferin. The light intensity emitted is directly proportional to the concentration of ATP present in the cell sample (Crouch, et al 1993).

4.3.1 Aims

The aim was to investigate the metabolic activity of FB_1- and SF-treated Jurkat cells by measuring ATP concentration.

4.3.2 Materials and Methods

4.3.2.1 Materials

The CellTitre-Glo® Assay was purchased from Promega (Madison, USA).

4.3.3.2 Method

The CellTitre-Glo® reagent was prepared (See Appendix D). Approximately 1.0 x 10^4 cells/well in 50µl of PBS were aliquotted to an opaque polystyrene flat-bottomed 96 well plate. A blank sample was set up as a negative control, containing only PBS. This was done to correct background luminescence.

50µL CellTitre-Glo® Reagent was added to each well and the plate was agitated briefly in order to mix the cell suspension with the assay reagent. The plate was then incubated at RT

for 1 h. Following incubation, the plate was agitated again and placed in a GloMax Multi Detection System. The luminescence from each sample was measured using the CellTitre-Glo ^{TM} assay software.

4.3.3 Results and Discussion

Results for the ATP assay was expressed in Relative Light Units (RLU).

The highest value of 8.17 RLU was observed in SF-treated cells, which was significant when compared to control, FB_1 and combination treatments [$p<0.05$]. Combination treatment was 4.17 RLU and showed no significance against FB_1 alone, but significance when compared to all other treatments [$p<0.05$]. FB_1 had a value of 2.28 RLU, and showed significance only against SF-treated cells. The control treatment was measured at 0.22 RLU (See Figure 4.5).

It has been reported that apoptosis is an energy-dependent process; hence it is heavily reliant on both the presence of ATP and functioning mitochondria. Active nuclear transport is needed for the transfer of large molecules across the nuclear membrane during Fas-mediated apoptosis, as death signals are transmitted from the cytoplasm to the nucleus. Additionally, in Jurkat cells the utilisation of ATP is necessary for nuclear cell fragmentation and chromatin condensation (Bradbury, *et al.* 2000).

D-pinitol is an active constituent of SF, and has anti-hyperglycaemic properties. It has been proposed that D-pinitol exerts this action by interacting with the cellular signalling pathway linking insulin to glucose transport (Bates, 2000), enabling it to improve glucose metabolism and increase cellular energy as a result of an increase in oxidative phosphorylation (Sivkumar, 2009). This action may have contributed to the high ATP found in SF-treated cells. Sethi, *et al.* (2008) demonstrated that pinitol was capable of inhibiting NF-κB activation, an action that was not cell-type specific. This inhibition led to the down-regulation

of gene products associated with cell proliferation, including cyclin D1 and c-myc; and cell survival, including Bcl-2 and Bcl-xL, thus resulting in increased apoptosis (Sethi, *et al.* 2008). This is reflected in the data, as the bioluminescent assay shows significantly high levels of ATP in SF-treated cells, compared with all other treatments [$p<0.05$]. This correlates with caspase-3 assay data, which indicates high levels of caspase-3 activity in SF-treated cells. It was also observed that the combination treatment was significantly lower than cells treated with SF alone, indicating that FB_1 may have played an antagonistic role to the action of SF. However, ATP in combination treatment was higher than in cells treated with FB_1 alone, albeit not significant, which again highlighted the action of D-pinitol in ATP production (See Figure 4.5).

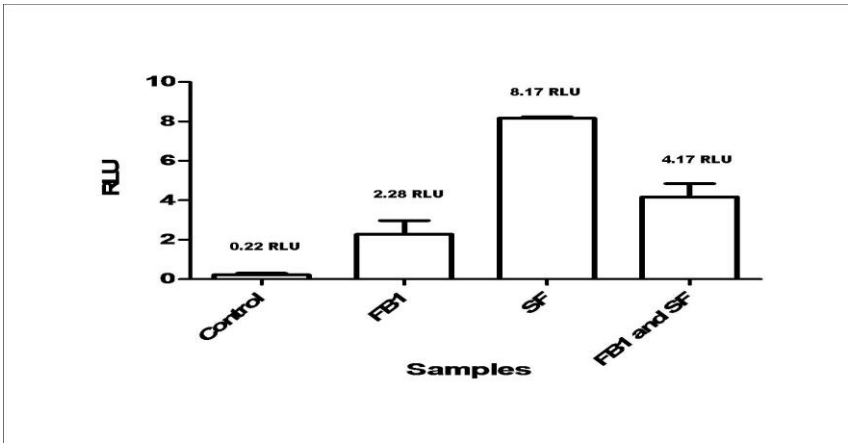

Figure 4.5 – Adenosine Tri Phosphate Assay results for treatment samples

(RLU – Relative Light Units)

CHAPTER 5

SPECTROPHOTOMETRIC ANALYSIS OF REACTIVE NITROGEN AND OXYGEN SPECIES IN FUMONISIN B_1 AND *SUTHERLANDIA FRUTESCENS* TREATED JURKAT CELLS

5.1 Nitric Oxide Assay

Nitric Oxide (NO) is most commonly known as a reactive nitrogen species that combines with superoxides to form powerful oxidants that cause cellular damage. However, it can also scavenge superoxides by forming non-reactive species, thus possessing both cytotoxic and cytoprotective activity, depending on the concentration levels of NO (Riganti, et al 2003).

The conversion of L-ARG to L-citrulline is dependent on NO, which has also been shown to regulate apoptosis via S-nitrosylation (Liu, *et al.* 2010; Iyer, *et al.* 2008).

Recent evidence indicates that NO activates a complex network of responses leading to apoptosis via mitochondrial, death receptor, p38/MAPK, and glyceraldehyde-3-phosphate dehydrogenase (GAPDH)-Siah1 cascades. The transient and volatile nature of NO makes it unsuitable for most convenient detection methods; however, two stable breakdown products, nitrate (NO_3) and nitrite (NO_2) can be easily detected by photometric means.

5.1.1 Aims

The aim was to investigate NO levels in Jurkat cells pre-treated with FB_1 and SF, by measuring NO_3 and NO_2 products using spectrophotometry.

5.1.2 Materials and Methods

5.1.2.1 Materials

Production of NO was measured under acidic conditions as NO_2, using the Griess Reagent System with Vanadium Chloride (VCl_3), 2% sulphanilamide (SULF), 0.1% *N*-1-napthylethylenediamine dihydrochloride (NEDD) (Promega, Madison, WI). Reagents were prepared according to the procedure discussed in Appendix C.

5.1.2.2 Method

Pre-treated Jurkat cell supernatant (SF, FB_1, and combination treatment) were diluted 1:5 with dH_2O. 100µL of sample was added to each well of a microtitre plate, followed by 100µL VCl_3. SULF (50 µL) and NEDD (50 µL) were then rapidly added to each well. Sodium nitrite standards (100 µL: 0 µM – 200 µM) were prepared (Appendix C) and added to the respective wells and the plate was incubated for 45 minutes in the dark at 37^{o}C. The optical density was measured at 540/690 nm, by a spectrophotometric plate reader (Bio-Tek µQuant)

Data Analysis

. A standard curve was derived using the nitrite standards (0 µM – 200 µM) and the NO concentration in each sample was extrapolated from the equation.

Statistical Analysis

Statistical significance was determined using One-Way Analysis of Variance (ANOVA) and the Bonferroni post test on GraphPad Prism v5.0 software (GraphPad Software Inc., La Jolla, USA) A probability value (p) of less than 0.05 ($p<0.05$) was considered statistically significant.

5.1.3 Results and Discussion

The NO concentration was determined by linear extrapolation from the standard curve and results were expressed in optical density values (OD).

Combination treatment had the highest OD value of 0.035 µM, but showed no significance when compared to SF, FB_1 and control treatments (See Figure 5.1). The value for SF-treated cells was measured at 0.032 µM and FB_1 had the lowest value at 0.019 µM, with both cell samples showing no significance when compared to all other treatments. The control treatment had a value of 0.033 µM (See Figure5.1). The release of TNF-α and other signalling molecules can result in an upregulation of iNOS, causing an increase in NO synthesis (Kim *et al.* 2001). The similar values of NO concentration between SF-treated cells and the control indicated that SF at the IC_{50} concentration used in this assay (0.91mg/ml) had little impact on NO synthesis. Only FB_1 appeared to have a negative effect on NO concentration. This may possibly be due to the ability of FB_1 to alter the TNF-α response.

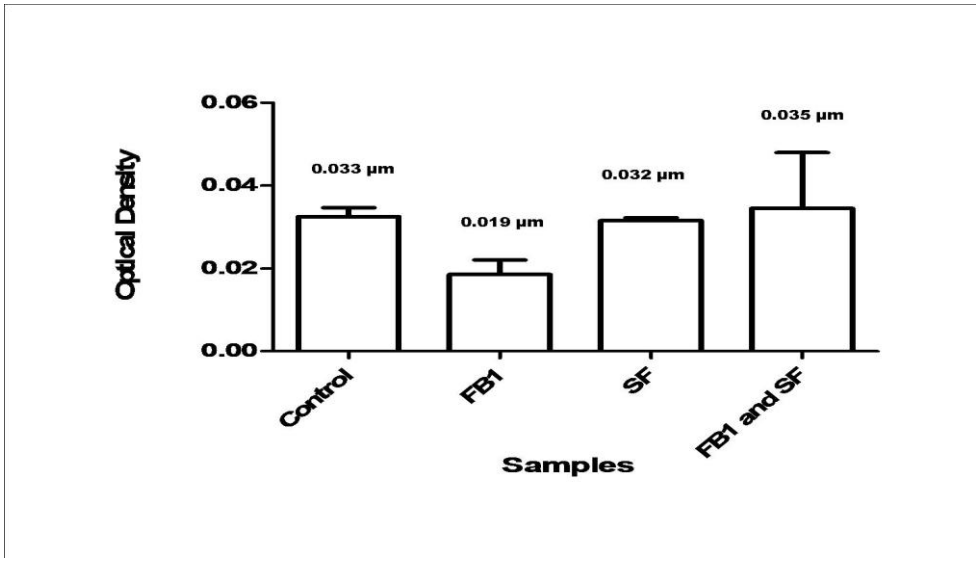

Figure 5.1: Reactive Nitrogen Species Assay results for treatment samples.

The apoptotic effect of NO has been shown to be cell-type specific and dependent on factors such as the presence of antioxidants. Apoptosis induced by NO in Jurkat cells have been observed to occur via the intrinsic/mitochondrial pathway, involving cytochrome c release into the cytosol, caspase-9 and ultimately caspase-3 activation, followed by the disruption of mitochondrial lipid synthesis (cardiolipin) Ushmorov *et al.* (1999).

Based on caspase-9 assay data, the mitochondrial pathway did not appear to be the key apoptotic pathway in SF-treated cells; therefore NO may not have played a significant role in SF- induced apoptosis, but may have still contributed to the observed caspase-9 activation.

5.2 Thiobarbituric Acid Reactive Substances (TBARS)

Malondialdehyde (MDA), a by-product of lipid peroxidation, is a highly reactive aldehyde capable of covalently bonding to protein, DNA and phospholipids, resulting in their inactivation (Houglum, *et al.* 1990). Several other reactive aldehydes and lipid peroxides are produced during lipid peroxidation, and the thiobarbituric acid-reactive substance TBARS assay is utilized to quantify these reactive substances within the tested sample. The basic principle of the assay involves the binding of reactive aldehydes and other substances to thiobarbituric acid to form a 1:2 adduct, which can be measured by spectrophotometry (Meagher, *et al.* 2000).

5.2.1 Aims

The aim was to investigate the levels of lipid peroxidation in FB_1 and SF-treated Jurkat cells.

5.2.2 Materials and Methods

5.2.2.1 Materials

Oxidative damage occurring in Jurkat cells was assessed using the TBARS assay.

5.2.2.2 Methods

Jurkat cells were centrifuged (24^0C; 400g; 10 min) and 500 µL of the supernatant was dispensed into glass tubes. A positive control of 1% MDA was prepared, as well as a blank negative control. To each glass tube, 200 µL of 7% H_2PO_3 was added, followed by 400 µL of

thiobarbituric acid (1%, w/v)/ 0.1 mM butylated hydroxytoluene solution. To the negative control, 400 µL of 3 mM HCl was added. The solution was adjusted to pH 1.5 and placed in a water bath at 100^0 C for 15 min. The samples were allowed to cool to RT, and 1500 µL of butanol was added to each tube. 500 µL of each sample was transferred to eppendorf tubes and centrifuged (24^0C 400 *g*, 6 min). Following centrifugation, 200 µL of the butanol phase from each sample (including controls) was aliquotted into a microtitre plate. The optical density was measured at 532/600 nm, by a spectrophotometric plate reader (Bio-Tek µQuant).

Statistical Analysis

Statistical significance was determined using One-Way Analysis of Variance (ANOVA) and the Bonferroni post test on GraphPad Prism v5.0 software (GraphPad Software Inc., La Jolla, USA) A probability value (p) of less than 0.05 [$p<0.05$] was considered statistically significant.

5.2.3 Results and Discussion

The TBARS concentration was expressed in optical density values (OD).

Levels of TBARS in FB_1 treated cells had an OD value of 1.95, which was significantly higher compared to control and SF treated cells [$p<0.05$]. Combination treatment had a significantly higher value when compared to treatment with FB_1 alone (2.58, [$p<0.05$]). There was no significant difference between SF and control treatments (0.252 vs. 0.277) (See Figure 5.2)

Lipid peroxidation is essentially the cyclic oxidation, or removal of hydrogen atoms from lipids by a free radical. Reactive species generally contain one or more unpaired electrons and is therefore sufficiently reactant to extract hydrogen atoms from fatty acid side chains.

The more double bonds present in the fatty acid side chain, the more effective the reactive species is at removing the hydrogen atom.

Lipid peroxidation occurs predominantly in cellular membranes, which results in membrane permeability, loss of membrane function, and the destabilising of membrane-bound receptors and enzymes (Abel, *et al.* 1998, Halliwell, *et al.* 1993).

The sphingolipid ceramide is linked to the induction of nitro-oxidative stress, through the generation of reactive species $O_2^{\cdot}$ and NO (Cuzzocrea, *et al.* 2008). The action of ceramide synthase is blocked by FB_1, preventing ceramide production (Ribiero, *et al.* 2010). Thus in theory, FB_1 should limit the presence of reactive species, however, FB_1 induces oxidative stress (Rumora, *et al.* 2007), and evidence also suggest a role for FB_1 in lipid peroxidation (Abel, *et al.* 1998, Stockmann-Juvala, *et al.* 2004). Hence FB_1 induces lipid peroxidation via an alternative mechanism, which may involve increasing molecular oxygen transport close to the surface of cell membranes, potentially accelerating oxidative reactions and ROS generation in the hydrophobic region of the membrane (Yin, et. al 1998). The data suggests that FB_1 contributed significantly to lipid peroxidation/oxidative stress. Data from SF-treated cells indicated that SF may have a scavenging effect on reactive species, rather an inducing one, at least when in combination with FB_1. The combination treatment data shows that FB_1 also appeared to significantly reverse the antioxidant protection afforded by SF. This correlates with Annexin data, and supports the hypothesis that PS oxidation is limited by the antioxidant activity of SF, which is reversed by FB_1.

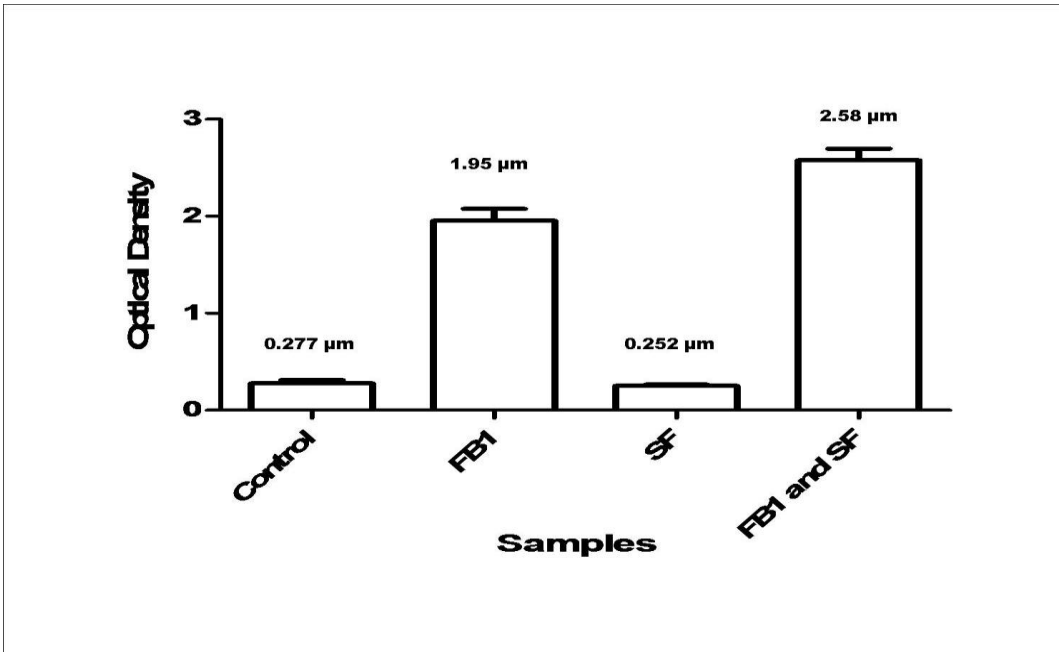

Figure 5.2: Thiobutyric acid reactive species (TBARS) assay results for treatment samples.

CONCLUSION

Proliferation in Jurkat cells was induced by FB_1, which supports existing evidence for its carcinogenic properties. Proliferation was time-dependent however, and cells became cytotoxic after 48 h. Cell proliferation may have been stimulated due to the ability of FB_1 to alter sphingolipid metabolism. Further investigation such as sphingoid base quantification via HPLC analysis would provide more insight into this proposed mechanism. Cytotoxicity may be a result of FB_1-induced reactive species generation.

Mitochondrial depolarization in Jurkat cells is induced by FB_1, owing to its generation of reactive species that react with thiobarbituric acid, although this did not appear to be a main indicator of apoptosis. An antagonistic relationship existed between FB_1 and SF in caspase-3/7, and -8 activities, but a synergistic one in caspase-9, indicating FB_1-induced apoptosis may occur via the mitochondrial pathway. Apoptosis in Jurkat cells was induced by SF maybe via the death-receptor mediated extrinsic pathway, as characterized by caspase-8 activity, which correlates with its status as an anti-cancer agent. The depletion of GSH by FB_1 may be enhanced by SF due to the action of weak acid GABA, although further studies using higher concentrations of SF would need to be conducted in order to confirm this. The action of D-pinitol may contribute to increasing ATP in SF-treated Jurkat cells, which may also contribute to apoptotic activity, as apoptosis is an ATP-dependent process. Based on data from this study, both SF and FB_1 appear to antagonize each other in some cases, for example in apoptotic activity as measured by caspase data; and act synergistically in others as exemplified by GSH depletion. This can be problematic if both are ingested together, hence this area of research warrants further investigation into the effects of SF and FB_1 on human T-lymphocytes, as well as other cell lines and in vivo studies.

REFERENCES

1. Abel, S., Gelderblom WC. (1998). Oxidative damage and fumonisin B_1 -induced toxicity in primary rat hepatocytes and rat liver in vivo. Toxicology 131, 121-131.
2. Agledal, L., Niere, M., Ziegler, M. (2010). The phosphate makes a difference: cellular functions of NADP. Redox Report, 15(1); 2-10.
3. Akaogi, J., Barker, T., Kuroda, Y., Nacionales, D., Yamasaki, Y., Stevens, B., Reeves, W., and Satoh, M. (2006). Role of non-protein amino acid l-canavanine in autoimmunity. Autoimmunity Reviews 5(6), 429-435.
4. Astoul, E., Edmunds, C., Cantrell, D.A., Ward, S.G., (2001) PI 3-K and T-cell activation: limitations of T-leukemic cell lines as signaling models. Trends in Immunology. 22, 490–496.
5. Barry, M, Bleackley, RC (2002). Cytotoxic T lymphocytes: all roads lead to death. Nature Reviews Immunology;2:401–9
6. Bates, S.H, Jones, R.B. Bailey, C.J (2000) Insulin-like effect of Pinitol, British Journal of Pharmacology, 130, 1944-1948
7. Behrens, A, S. M. Wagner, E.F (1999). Amino-terminal phosphorylation of c-Jun regulates stress induced apoptosis and cell proliferation. Nature Genetics 21, 326-329.
8. Bence, AK, Worthen, DR, Adams VR, Crooks PA, (2002) The antiproliferative and immunotoxic effects of L-canavanine and L-canaline, Anticancer Drugs.13(3):313-20.
9. Bensaad, K., Tsuruta, A., Selak, M., Vidal, M., Nakano, K., Bartrons, R., Gottlieb, E., and Vousden, K. (2006). TIGAR, a p53-Inducible Regulator of Glycolysis and Apoptosis. Cell 126(1), 107-120.
10. Bernhard, D.S.W., Crazzolara, R. Tinhofer, I. Kofler, R. Csordas, A (2003). Enhanced MTT-reducing activity under growth inhibition by resveratrol in CEM-C7H2 lymphocytic leukemia cells. Cancer Letters 195, 193-199.
11. Berridge, M.V, T. A. S., McCoy K.D, Wang R (1996). The biochemical and cellular basis of cell proliferation assays that use tetrazolium salts. Biochemica 4, 14-19.
12. Bhandari, N, R. P., Sharma (2002). Modulation of selected cell signaling genes in mouse liver by fumonisin B1. Chemico-Biological Interactions 139, 317-331.
13. Bhatnagar, D., Cleveland, TE. Dowd, PF., Desjardins, AE., Cotty, PJ, (2003) United States Department of Agriculture-Agricultural Research Service research on pre-harvest prevention of mycotoxins and mycotoxigenic fungi in US crops. Pest Management Science, 59 (6-7), 629-42

14. Bradbury, D.A, Simmons T.D, Slater, K.J, Crouch, S.P.M (2000) Measurement of the ADP:ATP ratio in human leukaemic cell lines can be used as an indicator of cell viability, necrosis and apoptosis. Journal of Immunological Methods 240, 79–92
15. Brand, MD. Chappell, JB (1973). Permeability of mitochondria from rat liver and rat brain to GABA. Journal of Neurochemistry. 22:47–51
16. Buchakjian, M. R., and Kornbluth, S. (2010). The engine driving the ship: metabolic steering of cell proliferation and death. Nature Reviews Molecular Cell Biology 11(10), 715-727.
17. Carretta, M., Alarcon, P., Jara, E., Solis, L., Hancke, J., Concha, I., Hidalgo, M., and Burgos, R. (2009). Andrographolide reduces IL-2 production in T-cells by interfering with NFAT and MAPK activation. European Journal of Pharmacology 602(2-3), 413-421.
18. Chelule, P.K, G. N., Dutton, M.F. Chuturgoon, AA (2001). Exposure of rural and urban populations in KwaZulu Natal, South Africa to fumonisin B1 in maize. Environmental Health Perspectives 109, 253-256.
19. Chinkwo, K. (2005). Sutherlandia frutescens extracts can induce apoptosis in cultured carcinoma cells. Journal of Ethnopharmacology 98(1-2), 163-170.
20. Choi B, Pae HO, Jang, SI, Kim, YM, Chung, HT (2002). Nitric Oxide as a Pro-apoptotic as well as Anti-apoptotic Modulator. Journal of Biochemistry and Molecular Biology 35 (1), 116-126
21. Crimi, M., and Esposti, M. D. (2010). Apoptosis-induced changes in mitochondrial lipids. Biochimica et Biophysica Acta (BBA) - Molecular Cell Research.
22. Crimi, M.E.M.D. (2010). Apoptosis: induced changes in mitochondrial lipids. Biochimica et Biophysica Acta xxx, xxx-xxx.
23. Crouch, S, Kozlowski, R. Slater. K. (1993) The use of ATP bioluminescence as a measure of cell proliferation and cytotoxicity. Journal of Immunological Methods 160:8188
24. Cuzzocrea, S., Di Paola, R., Genovese, T., Mazzon, E., Esposito, E., Crisafulli, C., Bramanti, P., and Salvemini, D. (2008). Anti-Inflammatory and Anti-Apoptotic Effects of Fumonisin B1, an Inhibitor of Ceramide Synthase, in a Rodent Model of Splanchnic Ischemia and Reperfusion Injury. Journal of Pharmacology and Experimental Therapeutics 327(1), 45-57.
25. Dawnlinsley, M., Ekinci, F., Ortiz, D., Rogers, E., and Shea, T. (2005). Monitoring

thiobarbituric acid-reactive substances (TBARs) as an assay for oxidative damage in neuronal cultures and central nervous system. Journal of Neuroscience Methods 141(2), 219-222.

26. Debabrata, Mandal. A. M., Pradeep, Das Manikuntala, Kundu, Joyoti, Basu (2005). Fas-, caspase 8-, and caspase 3-dependent signalling regulates the activity of the aminophospholipid translocase and phosphatidylserine externalization in human erythrocytes. Journal of Biological Chemistry 280, 34960-34967.
27. Dragan, Y, B. W., Cohen, S. Goldsworthy, T Hard, G. Howard, P Riley, R. Voss, K. (2001). Implications of Apoptosis for Toxicity, Carcinogenicity, and Risk Assessment- Fumonisin B1 as an Example. Society of Toxicology. 61, 6-17.
28. Dugyala, R.R, R. P. Sharma, Tsunoda, M. Riley, R.T (1998). Tumour Necrosis Factor-α as a Contributor in Fumonisin B1 Toxicity. Journal of Pharmacology and Experimental Therapeutics 285, 317-324.
29. Dvorak, NJ. Riley, RT Harris, M. McGregor, JA (2008) Fumonisin mycotoxin contamination of corn-based foods consumed by potentially pregnant women in southern California. Journal of Reproductive Medicine 53 (9):672-6.
30. Ehrlich, V.D.F. Uhl, M. Steinkellner, H. Zsivkovit, Knasmueller S. (2002). Fumonisin B_1 is genotoxic in human derived hepatoma (HepG2) cells. Mutagenesis 17, 257-260.
31. Elmore, S (2007). Apoptosis: A Review of Programmed Cell Death. Toxicology Pathology; 35 (4), 495-516
32. Elnekeety, A. Elkholy, W. Abbas, N. Ebaid, A. Amra, H. Abdelwahhab, M. (2007). Efficacy of royal jelly against the oxidative stress of fumonisin in rats. Toxicon 50(2), 256-269.
33. Fadok, VA. Cathelineau, A. Daleke, DL. Henson, PM. Bratton, D. (2000). Loss of Phospholipid Asymmetry and Surface Exposure of Phosphatidylserine is required for Phagocytosis of Apoptotic Cells by Macrophages and Fibroblasts. Journal of Biological Chemistry; 276, 1071-1077
34. Fadok, V.A.H.P. (2003). Apoptosis: giving phosphatidylserine recognition an assist – with a twist. Current Biology 13, 655-657.
35. Fan, Z. Beresford, PJ. Oh, D.Y. Zhang, D. Lieberman, J (2003). Tumour suppressor NM23-H1 is a granzyme Activated DNase during CTL- mediated apoptosis, and the nucleosome assembly protein SET is its inhibitor. Cell; 112:659–72.
36. Fariss, M.W, Patel, M Van Houten, B. Orrenius, S. (2005). Role of Mitochondria in

Toxic Oxidative Stress. Molecular Interventions 5(94-111).

37. Fernandes, A. Cromarty, A. Albrecht, C. and Jansenvanrensburg, C. (2004). The antioxidant potential of *Sutherlandia Frutescens*. Journal of Ethnopharmacology 95(1), 1-5.
38. Gelderblom, W.C.A Jaskiewicz K, M. W. F. O., Thiel, P.G. Horak, R.M. Vleggaar, R. Kriek, N.P.J. (1988). Fumonisins--novel mycotoxins with cancer-promoting activity produced by *Fusarium moniliforme*. Applied and Environmental Microbiology 54(7), 1806-1811.
39. Gelderblom, W.C.A, S. E. Marasas, W.F.O. Farber, E (1992). The cancer-initiating potential of the fumonisin B mycotoxins. Carcinogenesis 13(3), 433-437.
40. Gopee, N. (2003). Fumonisin B1-induced apoptosis is associated with delayed inhibition of protein kinase C, nuclear factor-κB and tumour necrosis factor α in LLC-PK1 cells. Chemico-Biological Interactions 146(2), 131-145.
41. Green, D. (1998). Apoptotic Pathways - The Roads to Ruin. Cell 94, 695-698.
42. Greenwood, M. Kreider, R.B. Rasmussen, C. Almada, A.L. Earnest, C.P. (2001). D-pinitol augments whole body creatine retention in man. Journal of Exercise Physiology 4, 41–47.
43. Halliwell, B.C.S. (1993). Lipid peroxidation- its mechanism, measurement, and significance. American Journal of Clinical Nutrition 57, 715-725.
44. Harnett, S. Oosthuizen, V. and Vandeventer, M. (2005). Anti-HIV activities of organic and aqueous extracts of and. Journal of Ethnopharmacology 96(1-2), 113-119.
45. Hassan, A. M. Mohamed, S. R. El-Nekeety, A. A. Hassan, N. S. Abdel-Wahhab, M. A. (2010). *Aquilegia vulgaris L*. extract counteracts oxidative stress and cytotoxicity of fumonisin in rats. Toxicon 56(1), 8-18.
46. Hill, M.M. Duriez, P.J. Creagh, E.M. Martin, S.J (2004). Analysis of the composition, assembly kinetics and activity of native Apaf-1 apoptosomes. EMBO Journal 23, 2134-2145.
47. Holman, G.D. Kasuga, M. (1997). From receptor to transporter: insulin signalling to glucose transport. Diabetologia, 40, 991 -1003
48. Honglin, Li. Chi-jie Xu, Junying Yuan (1998). Cleavage of BID by Caspase 8 Mediates the Mitochondrial Damage in the Fas Pathway of Apoptosis. Cell 94, 491-501.
49. Houglum, K. Filip, M. Witztum, J.L. Chojkier, M. (1990) Malondialdehyde and 4-

Hydroxynonenal Protein Adducts in Plasma and Liver of Rats with Iron Overload. Journal of Clinical Investigation 86; 1991-1998

50. Huerta, S. Goulet, E. Huertayepez, S. and Livingston, E. (2007). Screening and Detection of Apoptosis. Journal of Surgical Research 139(1), 143-156.
51. Idriss, H.T. and Naismith, J.H. (2000). TNFα and the TNF receptor superfamily: structure-function relationship(s). Microscopy Research and Technique. *50*, 184–195
52. Iyer, A.K.V. Azad, N. Wang, L. and Rojanasakul, Y. (2008). Role of S-nitrosylation in apoptosis resistance and carcinogenesis. Nitric Oxide 19(2), 146-151.
53. J.W, A. (2001). Structure, Synthesis, and Biosynthesis of Fumonisin B1 and Related Compounds. Environmental Health Perspectives 109, 245-249.
54. Jiang, J. Serinkan, BF. Tyurina, YY. Borisenko, GG. Mi, Z. Robbins, PD. Schroit, AJ. Kagan, V.E. (2003). Peroxidation and Externalization of Phosphatidylserine Associated with Release of cytochrome c from Mitochondria. Free Radical Biology and Medicine 35; 7, 814-825
55. Johnson, V. (2003). Increased susceptibility of renal epithelial cells to TNFα-induced apoptosis following treatment with fumonisin B1. Chemico-Biological Interactions 145(3), 297-309.
56. Jones, D.P (2006). Redefining oxidative stress. Antioxidant Redox Signaling 8:1865_1879.
57. Jones, C. C.-Z. J., Zhang, Y. Henderson, G. Dickman M (2001). Analysis of fumonisin B_1-induced apoptosis. Environmental Health Perspectives 109, 315-320.
58. Karvinen, J. (2002) Homogeneous time-resolved fluorescence quenching assay (LANCE) for caspase-3. Journal of Biomolecular. Screening. 7, 223–31.
59. Katerere, D.R. Eloff, J.N. (2005). Antibacterial and antioxidant activity of *Sutherlandia frutescens* (Fabaceae), a reputed Anti-HIV/AIDS phytomedicine. Phytotherapy Research 19(9), 779-781.
60. Kiang, J. G. Krishnan, S. Lu, X. Li, Y. (2007). Inhibition of Inducible Nitric-Oxide Synthase Protects Human T Cells from Hypoxia-Induced Apoptosis. Molecular Pharmacology 73(3), 738-747.
61. Kim, P. Petrosko, P. Billiar, T. (2001). The regulatory role of nitric oxide in apoptosis. International Immunopharmacology ,**1**:1421–1441.
62. Kirkham, P.A. Lam, E. Parkhouse, R.M.E. (2000). Ligation of the WC1 Receptor Induces T call growth arrest through FB_1-sensitive increases in Cellular Ceramide.

Journal of Immunology 165, 3564-3570.

63. Kischkel, F.C. Behrmann, I. Germer, M. Pawlita, M. Krammer, P.H, Peter, M.E. (1995). Cytotoxicity-dependent APO-1 (Fas-CD95)-associated proteins form a death-inducing signalling complex (DISC) with the receptor. EMBO Journal 14, 5579-5588.
64. Korb, V.C. Chuturgoon, A.A. (2010). Apoptosis-promoting effects of Sutherlandia frutescens extracts on Normal Human Lymphocytes in Vitro. South African Journal of Science 106, 64-69.
65. Legrand, O. Perrot, JY. Simonin, G. Baudard, M., Marie, JP. (2001) JC-1: a very sensitive fluorescent probe to test Pgp activity in adult acute myeloid leukemia. Blood 97, 502-508
66. Levy, B. (2004). Comparative effects of vasopressin, norepinephrine, and L-canavanine, a selective inhibitor of inducible nitric oxide synthase, in endotoxic shock. AJP: Heart and Circulatory Physiology 287(1), H209-H215.
67. Li, C. Hanigan, C.L. Hofseth, L.J. Trudel, L.J. Harris, C.C. Wogan, G.N. (2004). Apoptotic signalling pathways induced by nitric oxide in human lymphoblastoid cells expressing wild-type or mutant p53. Cancer Research 64, 3022-3029.
68. Liu, B. (2002). The Effects of Mycotoxins, Fumonisin B1 and Aflatoxin B1, on Primary Swine Alveolar Macrophages. Toxicology and Applied Pharmacology 180(3), 197-204.
69. Liu, M. H. J. Huang, L. Huang, X. Heibeck, HT. Zhao, R. Pasa-Tolic, L. Smith, R. Kai Fu, Y. Zhang, Z. Hinrichs, S. Ding, S. (2010). Site-Specific Proteomics Approach for Study Protein S-Nitrosylation. Analytical Chemistry.
70. Liu, Y.P. Kimura, H. Schubert, D. (1997). Mechanism of Cellular 3- (4,5-Dimethylthiazol-2-yl) -2,5-Diphenyltetrazolium Bromide (MTT) Reduction. Journal of Neurochemistry 69 581 —593.
71. Locksley, R.M. Lenardo, M.J. (2001). The TNF and TNF Receptor Superfamilies-Integrating Mammalian Biology. Cell 104, 487-501.
72. Luongo, D. Severino, L. Bergamo, P. De Luna, R. Lucisano, A. Rossi, M. (2006) Interactive effects of Fumonisin B_1 and α zearalenol on proliferation and cytokine expression in Jurkat T cells, Toxicology in Vitro 20, 1403-1410
73. Maenetje, P. W. de Villiers, N. Dutton, M. F. (2008). The Use of Isolated Human Lymphocytes in Mycotoxin Cytotoxicity Testing. International Journal of Molecular Sciences 9(8), 1515-1526.

74. Mander, M. Ntuli, L. Diederichs, N. Mavundla, K. (2007) Economics of the Traditional Medicine Trade in South Africa – Chapter 13. South African Health Review, Health Systems Trust.
75. Martinvalet, D. Zhu, P. Lieberman, J. (2005). Granzyme A Induces Caspase-Independent Mitochondrial Damage, a Required First Step for Apoptosis. Immunity 22(3), 355-370.
76. Massimo, Crimi. (2010). Apoptosis-induced changes in mitochondrial lipids. Biochimica et Biophysica Acta.
77. Meagher, EA, Fitzgerald, GA. (2000) Indices of Lipid Peroxidation in vivo: strengths and limitations. Free Radical Biological Medicine; 28:1745–50.
78. Mills, E., Cooper, C. Seely, D. (2005). African herbal medicines in the treatment of HIV: Hypoxis and Sutherlandia. An overview of evidence and pharmacology. Nutrition Journal 4(1), 19.
79. Neff, N. Reddy, T. Cell Growth Protocol for Jurkat Cell Line; Hudson Alpha/Caltech ENDCODE group; August 27th 2008
80. Ngondi, J. L. Oben, J. Etame, L. H. Forkah, D. M. and Mbanya, D. (2006). The effect of different combination therapies on oxidative stress markers in HIV infected patients in Cameroon. AIDS Research Therapy 3(1), 19.
81. O'Brien, M.A. *et al.* (2005) Homogeneous, bioluminescent protease assays: caspase-3 as a model. J. Biomolecular. Screening. 10, 137–48.
82. O, C. (2002). Sphingosine in apoptosis signaling. Biochimica et Biophysica Acta 1585, 153– 162.
83. Odhav, B. Adam, J.K. Bhola, K.D. (2008) Modulating effects of fumonisin B_1 and ochratoxin A on leukocytes and messenger cytokines of the human immune system, International Immunopharmacology, 8, 799-809
84. Ojewole, J. A. O. (2008). Anticonvulsant property of *Sutherlandia frutescens R. BR*. (variety Incana E. MEY.) [Fabaceae] shoot aqueous extract. Brain Research Bulletin 75(1), 126-132.
85. Ormerod, M.G (2000). Flow Cytometry: A Practical. 3rd ed. Oxford: Oxford University Press 1-27, 240,243
86. Ott, M. Gogvadze, V. Orrenius, S. Zhivotovsky, B. (2007). Mitochondria, oxidative stress and cell death. Apoptosis 12(5), 913-922.
87. Ott, M. Gogvadze, V. Orrenius, S. Zhivotovsky, B. (2007). Mitochondria, oxidative

stress and cell death. Apoptosis 12(5), 913-922.

88. Packer, L. Cadenas, E. (2007). Oxidants and antioxidants revisited. New concepts of oxidative stress. Free Radical Research 41(9), 951-952.
89. Paila, Y. D. Ganguly, S. Chattopadhyay, A. (2010). Metabolic Depletion of Sphingolipids Impairs Ligand Binding and Signaling of Human Serotonin1A Receptors. Biochemistry 49(11), 2389-2397.
90. Pallardo, F.V. Markovic, J. Garcia, JL. Vina, J. (2009). Role of Nuclear Glutathione as a key regulator of Cell Proliferation. Molecular Aspects of Medicine. 30; 77-85
91. Peng, L. Wang, B. Ren, P. (2005). Reduction of MTT by flavonoids in the absence of cells. Colloids and Surfaces B: Biointerfaces 45(2), 108-111.
92. Peng, L. Wang, B. and Ren, P. (2005). Reduction of MTT by flavonoids in the absence of cells. Colloids and Surfaces B: Biointerfaces 45(2), 108-111.
93. Peter, Kim. Patricia, Petrosko. Timothy, Billiar. (2001). The regulatory role of nitric oxide in apoptosis. International Immunopharmacology 1, 1421–1441.
94. Proskuryakov, S. (2003). Necrosis: a specific form of programmed cell death? Experimental Cell Research 283(1), 1-16.
95. Puga, I. (2005). A Polymorphism in the 3' Untranslated Region of the Gene for Tumour Necrosis Factor Receptor 2 Modulates Reporter Gene Expression. Endocrinology 146(5), 2210-2220.
96. Rahman, M. Pumphrey, JG. Lipkowitz, S. (2009) The TRAIL to Targeted Therapy of Breast Cancer. Advanced Cancer Research 103; 43-73
97. Rastogi, R.P. Sinha, R.P. (2009). Apoptosis - Molecular Mechanisms and Pathogenicity. EXCLI Journal 8, 155-181.
98. Ribeiro, D. H. B. Ferreira, F. L. da Silva, V. N. Aquino, S. Corrêa, B. (2010). Effects of Aflatoxin B1 and Fumonisin B1 on the Viability and Induction of Apoptosis in Rat Primary Hepatocytes. International Journal of Molecular Sciences 11(4), 1944-1955.
99. Riganti, C. Aldieri E, Bergandi, L. Miraglia, E. Costamagna, C. Bosia, A. Ghigo, D. (2003). Nitroarginine methyl ester and canavanine lower intracellular reduced glutathione. Free Radical Biology and Medicine 35(10), 1210-1216.
100. Rumora, L. Domijan, A. Grubisic, T. and Peraica, M. (2007). Mycotoxin fumonisin B1 alters cellular redox balance and signalling pathways in rat liver and kidney. Toxicology 242(1-3), 31-38.

101. Rumora, L. Kovacic, S. Rozgaj, R. Cepelak, I. Pepeljnjak, S. Grubisic, T.Z. (2002) Cytotoxic and genotoxic effects of fumonisin B1 on rabbit kidney RK13 cell line. Archives of Toxicology. 76, 55–61.

102. Salvioli, S. Ardizzoni, A. Franceschi, C. Cossarizza, A. (1997) JC-1, but not $DiOC_6(3)$ or rhodamine 123, is a reliable fluorescent probe to assess $\Delta\Psi$ changes in intact cells: implications for studies on mitochondrial functionality during apoptosis. Federation of European Biochemical Sciences 411, 77-82

103. Schimmer, A.D. (2004). Inhibitor of apoptosis proteins: translating basic knowledge into clinical practice. Cancer Research; 64: 7183–7190.

104. Schreck, R. Baeuerle, P.A (1991). Reactive oxygen intermediates as apparently widely used messengers in the activation of the NF-kappa B transcription factor and HIV-1. EMBO Journal 10, 2247-2258.

105. Schroeder, J.J. Xias, J. Liotta, D.C. Merrill, A.H. (1994). Disruption of Sphingolipid Metabolism and Stimulation of DNA synthesis by FB1. The Journal of Biological Chemistry 269, 3475-3481.

106. Schwerdt, G. Königs, M. Holzinger, H. Humpf, H. U. and Gekle, M. (2009). Effects of the mycotoxin fumonisin B1on cell death in human kidney cells and human lung fibroblasts in primary culture. Journal of Applied Toxicology 29(2), 174-182.

107. Scorrano, L. (2003). BAX and BAK Regulation of Endoplasmic Reticulum Ca2+: A Control Point for Apoptosis. Science 300(5616), 135-139.

108. Seefelder, W. (2003). Induction of apoptosis in cultured human proximal tubule cells by fumonisins and fumonisin metabolites. Toxicology and Applied Pharmacology 192(2), 146-153.

109. Sennepin, A. D. Charpentier, S. Normand, T. Sarré, C. Legrand, A. Mollet, L. M. (2009). Multiple reprobing of Western blots after inactivation of peroxidase activity by its substrate, hydrogen peroxide. Analytical Biochemistry 393(1), 129-131.

110. Serinkan, BF. Tyurina, YY. Babu, H. Djukic, M. Quinn, PJ. Schroit, A. Kagan, V (2004). Vitamin E Inhibits Anti-Fas-Induced Phosphatidylserine Oxidation but Does Not Affect Its Externalization during Apoptosis in Jurkat T Cells and their Phagocytosis by J774A.1 Macrophages. Antioxidants and Redox Signalling. 6; 2, 227-236

111. Sethi, G. Seok, Ahn K. Sung, B. (2008). Pinitol targets nuclear factor-κB activation pathway leading to inhibition of gene products associated with

proliferation, apoptosis, invasion and angiogenesis. Molecular Cancer Therapeutics 7:1604-1614

112. Sharma, N. He, Q. and Sharma, R. (2004). Sphingosine kinase activity confers resistance to apoptosis by fumonisin B in human embryonic kidney (HEK-293) cells. Chemico-Biological Interactions 151(1), 33-42.

113. Sharma, N. Suzuki, H. He, Q. and Sharma, R.P. (2006). Tumour necrosis factor α-mediated activation of c-Jun NH2-terminal kinase as a mechanism for fumonisin B1 induced apoptosis in murine primary hepatocytes. Journal of Biochemical and Molecular Toxicology 19(6), 359-367.

114. Sivakumar, S. and Subramanian, S.P. (2009). Pancreatic tissue protective nature of D-Pinitol studied in streptozotocin-mediated oxidative stress in experimental diabetic rats. European Journal of Pharmacology 622(1-3), 65-70.

115. Slee, E. A. (2000). Executioner Caspase-3, -6, and -7 Perform Distinct, Non-redundant Roles during the Demolition Phase of Apoptosis. Journal of Biological Chemistry 276(10), 7320-7326.

116. Smiley, S.T. Mottola-Hartshorn, C. Lin, M. Chen, A. Smith, T.W. Steele, G.D. Chen, L.B. (1991). Intracellular heterogeneity in mitochondrial membrane potentials. Cell Biology 88, 3671-3675.

117. Solomon, JC. Wei, LX. Fujita, T. Shi, Y.F. (2003). A novel role for sphingolipid intermediates in activation-induced cell death in T cells. Cell Death and Differentiation 10 193-202.

118. Sternfeld, T. Tischleder, A. Schuster, M. Bogner, J.R. (2009). Mitochondrial membrane potential and apoptosis of blood mononuclear cells in HIV-1 infected patients. HIV Medicine; 10: 512-519

119. Stockmann-Juvala, H. (2004). Fumonisin B1-induced toxicity and oxidative damage in U-118MG glioblastoma cells. Toxicology 202(3), 173-183.

120. Stockmann-Juvala, H. Alenius, H. Savolainen, K. (2008). Effects of fumonisin B1 on the expression of cytokines and chemokines in human dendritic cells. Food and Chemical Toxicology 46(5), 1444-1451.

121. Theumer, M. G. Cánepa, M. C. López, A. G. Mary, V.S. Dambolena, J.S. Rubinstein, H.R. (2010). Subchronic mycotoxicoses in Wistar rats: Assessment of the in vivo and in vitro genotoxicity induced by fumonisins and aflatoxin B1, and oxidative stress biomarkers status. Toxicology 268(1-2), 104-110.

122. Tice, R.R. Anderson, D. Burlinson, B. Hartmann, A. Kobayashi, H. Miyamae, Y. Rojas, E. Ryu, J.C. Sasaki, Y.F. (2000). Single cell gel or comet assay- guidelines for in vitro and in vivo genetic toxicology testing. Environmental and Molecular Mutagenesis 35, 206-221

123. Trapani, JA. Smyth, M.J. (2002). Functional significance of the perforin/granzyme cell death pathway. Nature Reviews Immunology; 2:735–47.

124. Ushmorov, A.F.R. Lehmann, V. Dröge, W. Schirrmacher, V. Umansky, V (1999). Nitric Oxide-Induced Apoptosis in Human Leukemic Lines Requires Mitochondrial Lipid Degradation and Cytochrome C Release. Blood 93 2342-2352.

125. Vandenabeele, P.D.W. Beyaert, R. Fiers, W (1995). Two tumour necrosis factor receptors - structure and function. Trends in Cell Biology 5, 392-399.

126. Vanwyk, B. Albrecht, C. (2008). A review of the taxonomy, ethnobotany, chemistry and pharmacology of Sutherlandia frutescens (Fabaceae). Journal of Ethnopharmacology 119(3), 620-629.

127. Visconti, A. Boenke, A. Doko, MB. Solfrizzo, M. Pascale, M. (1995) Occurrence of fumonisins in Europe and the BCR--measurements and testing projects, Natural Toxins. 1995;3 (4):269-74

128. Ware, C.F. Vanarsdale, T.L. Andrews, J.L. Grayson, M.H. Jerzy, R. Smith, C.A. Goodwin, R.G. (1991). TNF Receptor Expression in T-Lymphocytes Journal of Immunology 147, 4229-4238.

129. Wattenberg, F. Badria, F.A. (1996). Activation of Mitogen-Activated Protein Kinase by the Carcinogenic Mycotoxin Fumonisin B1. Biochemical and Biophysical Research Communications 227, 622-627.

130. Winrow, V.R. Winyard, P.G. Morris, C.J. Blake, D.R. (1993) Free radicals in inflammation: second messengers and mediators of tissue destruction. British Medical Bulletin 49, 506–522.

131. Yang, S. (2003). Transcriptional regulation by the MAP kinase signaling cascades. Gene 320, 3-21.

132. Yin, J.J. Eppley, R. Page, S.W. Sphon, J.A. (1998). Effects of fumonisin B1 on lipid peroxidation in membranes. Biochimica et Biophysica Acta 134-142.

APPENDIX

Appendix A

Preparation of *Sutherlandia frutescens* (SF) stock solution

Ten 300mg (total mass 3000mg) SF tablets were crushed with a pestle and mortar and subjected to polar solvent extraction of active ingredients in 22ml of 70% Ethanol for 4 h at RT. Subsequent to extraction, the particular matter was centrifuged for 10 min at 400g at RT.

The stock solution of SF was calculated as: 3000mg/22mL = 136.36mg/mL

The IC_{50} value for SF was obtained from literature (Tai, *et al.* 2004) as a 1/150 dilution of the stock solution, which was a value of 0.91mg/mL.

This IC_{50} concentration of SF was used for all further treatments of Jurkat cells.

Appendix B

Caspase-Glo® 3/7, 8 and 9 reagent preparations

Caspase-Glo® 3/7 Buffer and lyophilized Caspase-Glo® 3/7 substrate were equilibrated to RT before use.

Contents of the Caspase-Glo® 3/7 Buffer bottle was emptied into the bottle containing Caspase-Glo® 3/7 Substrate and mixed until the substrate was thoroughly dissolved to form the Caspase-Glo® 3/7 Reagent.

The freshly-prepared, reconstituted Caspase-Glo® 3/7 Reagent was stored at 4°C until ready for use. (N.B – It is not recommended to store freshly-prepared Caspase-Glo® 3/7 Reagent for longer than three days).
The same procedure was applied to Caspase-Glo® 8 and Caspase-Glo® 9 reagent.

CellTitre-Glo® Reagent Preparation

The lyophilised CellTitre-Glo® Substrate and CellTitre-Glo® Buffer were equilibrated to RT. The enzyme substrate mixture was reconstituted by adding the CellTitre-Glo® Buffer to a vial of CellTitre-Glo® Substrate and gently vortexed.

Appendix C

Nitrites and Nitrates (Reactive Nitrogen Species) Assay reagent preparations

i. VCl_3 – 100mg of VCl_3 was dissolved in 12.5mL of 1M HCl and filter-sterilised. Reagent was kept in foil and in the dark at 4^{o}C.

ii. *N*-1-napthylethylenediamine dihydrochloride (NEDD) (0.1%) – 10mg NEDD was dissolved in 10mL dH_2O

iii. Sulphanilamide (SULF) (2%) – 200mg SULF was dissolved in 10mL of 5% HCl (3mL 1M HCl, + 15mL dH_2O) and stirred on a hot plate. Reagent was kept in foil and in the dark at 4^{o}C.

iv. Standards – 6.06mg Sodium Nitrite was dissolved in 30mL dH_2O and 200µM stock was made up to 10 standards ranging from 0 - 200µM.